


12-2023

DETERMINING THE EFFECTS OF GLYCOCALYX MODIFICATIONS ON THE ELECTROPHYSICAL PROPERTIES OF HUMAN MESENCHYMAL STEM CELLS

Rominna E. Valentine Ico
California State University - San Bernardino

Follow this and additional works at: <https://scholarworks.lib.csusb.edu/etd>

 Part of the [Biochemical and Biomolecular Engineering Commons](#), [Bioinformatics Commons](#), [Biological Engineering Commons](#), [Biology Commons](#), [Membrane Science Commons](#), and the [Systems Biology Commons](#)

Recommended Citation

Valentine Ico, Rominna E., "DETERMINING THE EFFECTS OF GLYCOCALYX MODIFICATIONS ON THE ELECTROPHYSICAL PROPERTIES OF HUMAN MESENCHYMAL STEM CELLS" (2023). *Electronic Theses, Projects, and Dissertations*. 1834.

<https://scholarworks.lib.csusb.edu/etd/1834>

This Thesis is brought to you for free and open access by the Office of Graduate Studies at CSUSB ScholarWorks. It has been accepted for inclusion in Electronic Theses, Projects, and Dissertations by an authorized administrator of CSUSB ScholarWorks. For more information, please contact scholarworks@csusb.edu.

DETERMINING THE EFFECTS OF GLYCOCALYX MODIFICATIONS ON THE
ELECTROPHYSICAL PROPERTIES OF HUMAN MESENCHYMAL STEM
CELLS

A Thesis
Presented to the
Faculty of
California State University,
San Bernardino

In Partial Fulfillment
of the Requirements for the Degree
Master of Science
in
Biology

by
Rominna Estefania Valentine Ico
December 2023

DETERMINING THE EFFECTS OF GLYCOCALYX MODIFICATIONS ON THE
ELECTROPHYSICAL PROPERTIES OF HUMAN MESENCHYMAL STEM
CELLS

A Thesis

Presented to the

Faculty of

California State University,

San Bernardino

by

Rominna Estefania Valentine Ico

December 2023

Approved by:

Dr. Nicole Bournias, Committee Chair, Biology

Dr. Daniel Nickerson, Committee Member, Biology

Dr. Tayloria N.G. Adams, Committee Member, Chemical and Biomolecular
Engineering, University California of Irvine

© 2023 Rominna Valentine Ico

ABSTRACT

Human mesenchymal stem cells (hMSCs) have gained popularity in clinical trials due to their multipotent differentiation characteristics, ability to secrete bioactive molecules, migrate into diseased or damaged tissues, and their immunosuppressive properties. HMSC cultures are heterogeneous, containing stem cells, partially differentiated progenitor cells, and fully differentiated cells. One of the major challenges with hMSCs therapeutic potential is the inability to select specific cell subpopulations due to an insufficient number of biomarkers. Often the biomarkers used, like those for fluorescence-activated cell sorting, are not sufficient to define hMSCs because they overlap with other cell types. Consequently, there is a need to develop alternative biomarkers and sorting technology to reduce hMSCs heterogeneity through cell identification and selection. Recently, electrophysiological properties such as membrane capacitance and cytoplasm conductivity have emerged as biomarkers to identify subsets of stem cells using dielectrophoresis (DEP), a label-free cell analysis technique. DEP uses electric fields to align ions around the surface of cells and induces cell movement. One key feature of the cell surface is the glycocalyx, a biointerface composed of glycolipids and glycoproteins surrounding the membrane of cells. This work focuses on modifying the cell-specific glycosylation patterns that make up the glycocalyx using treatments of either Kifunensine or N-Acetylglucosamine to further develop membrane capacitance and cytoplasm conductivity as contenders for label-free biomarkers. Measurements collected by

modifications made to the glycocalyx using DEP to investigate the contributions of the glycocalyx to membrane capacitance and cytoplasm conductivity. Adipose tissue, (AT) was assessed throughout this experiment to determine if the changes undergone by treatment and differentiation can be accessed. Transient slope, a new parameter from DEP measurements, is evaluated as a third potential label-free biomarker. Modified and unmodified hMSCs will be differentiated into adipocytes and osteocytes, and RT-qPCR analysis of differentiation-related genes was performed to determine if the glycocalyx impacts cell fate. The results demonstrate that DEP can be used as a good engineering tool that provides label-free biomarkers, membrane capacitance, cytoplasm conductivity, and transient slope, as identifiers of hMSCs subpopulations.

ACKNOWLEDGEMENTS

Funding sources for the completion of this experiment are listed below.

- National Science Foundation (NSF) CAREER Award under grant no. 2048221.
- California Institute of Regenerative Medicine (CIRM) Bridges scholarship award- January 2022 through December 2022.

DEDICATION

I would like to dedicate this thesis to all those who have supported me and embraced the idea of advancing research in stem cells. Your unwavering support has been instrumental in our pursuit of scientific knowledge and my commitment to making a difference. Together, we strive to contribute to the discovery of treatments and improve the lives of future generations. This dedication is a testament to our shared vision of fostering scientific progress and creating a positive impact on both the scientific community and the public at large.

TABLE OF CONTENTS

ABSTRACT	iii
ACKNOWLEDGEMENTS.....	v
LIST OF FIGURES	vii
CHAPTER ONE: INTRODUCTION	1
Motivation for Work.....	2
Specific Aims	3
Aim 1: Modify the Glycocalyx Using N-Acetylglucosamine (Glcnac) and Quantify the DEP Response, Membrane Capacitance, Cytoplasm Conductivity, and Biological Function.....	3
Aim 2: Modify the Glycocalyx Using Kifunensine (Kifu) and Quantify the DEP Response, Membrane Capacitance, Cytoplasm Conductivity, and Biological Functions.....	4
CHAPTER TWO: BACKGROUND	6
Heterogeneity of hMSCs.....	6
What is Dielectrophoresis (DEP)?	9
Cell Polarization and DEP Spectra	12
Glycocalyx of the Cell	15
CHAPTER THREE: MODIFYING THE GLYCOCALYX OF HUMAN MESENCHYMAL STEM CELLS.....	18
Materials and Methods.....	21
Cell Culture	21
hMSCs Differentiation.....	22
Reverse Transcriptase Quantitative Polymerase Chain Reaction (RT-qPCR)	23
Treatment.....	23

Histological Staining.....	24
Results and Discussion.....	25
GlcNAc and Kifu Treatments.....	25
Cell Differentiation Post- GlcNAc and Kifu Treatments	27
DEP Response and Glycocalyx Modification	27
Histological Staining Post GlcNAc and Kifu Treatments	29
Histological Stains and Glycocalyx Modification	30
DEP Characterization.....	33
CHAPTER FOUR: CONCLUSION	37
APPENDIX A: POSTER PRESENTATION DISPLAYS	40
APPENDIX B: CO-CULTURING HUMAN MESENCHYMAL STEM CELLS.....	44
Co-Culturing Cells.....	45
APPENDIX C: HUMAN MESENCHYMAL STEM CELL SORTING USING A CYTOCHIP	46
APPENDIX D: QPCR ANALYSIS OF DIFFERENTIATION AND TREATMENT OF HMSCS.....	51
Cycles Threshold (Ct) Data for Differentiation and Treatment Data.....	52
APPENDIX E: PUBLICATION RIGHTS FOR IMAGES DISPLAYED	57
REFERENCES	65

LIST OF FIGURES

Figure 1. Schematic of MSCs And Their Ability to Self-Renew, Repair, and Differentiate Into Different Cell Types.....	2
Figure 2. The Heterogeneity of MSCs	7
Figure 3. “Cell Surface and Transcriptomic Comparison of MSCs” from Different Tissues Types	8
Figure 4. Schematic of How Cell Polarization and DEP Response Function in Cells	11
Figure 5. Visual Representation of The Positive and Negative DEP Responses Based On Changes In Frequency	12
Figure 6. DEP Response Based on Frequency Changes.....	13
Figure 7. Representation of the Glycocalyx Complexity	17
Figure 8. Experimental Workflow For (A) AT-hMSCs Glycocalyx Modification Using Treatment of Either GlcNAc or Kifu (B) with 24-Hour Media Replacement.	19
Figure 9. Molecular Structure of N-GlcNAc.	20
Figure 10. Molecular Structure of Kifu.	20
Figure 11. EVOS XL (Thermo Fisher Scientific, Frederick, MD) Microscope Images (40x Magnification) of AT-hMSCs that Underwent 5-Day Treatment of GlcNAc or Kifu.....	26
Figure 12. Schematic of the Cell Surface with (A) No Treatment, (B) GlcNAc Treatment, and (C) Kifu Treatment.....	28

Figure 13. Keyence Microscope Images (20x Magnification) of AT-hMSCs that Underwent 5-Day Treatment of GlcNAc and then an 8-Day or 21-Day Differentiation. 31

Figure 14. EVOS XL (Thermo Fisher Scientific, Frederick, MD) Microscope Images (20x Magnification) of AT-hMSCs that Underwent 5-Day Treatment of Kifu and then an 8-Day or 21-Day Differentiation. 32

Figure 15. DEP Response of AT-hMSCs with (A) GlcNAc and Kifu Treatments, (B) GlcNAc Treatment with Adipocyte Differentiation (AD) and Osteoblast Differentiation (OD), (C) Kifu Treatment with AD and OS, and (D) Combination of All Treatment Conditions. (E) Provides Cell Size and Estimations of Cytoplasm Conductivity, Membrane Capacitance, and the Maximum Relative DEP Force. 35

CHAPTER ONE:

INTRODUCTION

Human mesenchymal stem cells (hMSCs) are important cells to study because of their multipotent differentiation characteristics (see Figure 1 below), ability to secrete bioactive molecules, migrate into diseased or damaged tissues, and their immunosuppressive properties. HMSC cultures are considered heterogeneous, containing stem cells, partially differentiated progenitor cells, and fully differentiated cells [1]. One of the major challenges with using hMSCs' therapeutic potential is the inability to select specific subpopulations due to an insufficient number of biomarkers [2]. Often the biomarkers used, like those for fluorescence-activated cell sorting, overlap with other cell-type phenotypes. Consequently, there is a need to develop alternative biomarkers and sorting technology to reduce hMSCs heterogeneity through cell identification and selection for potential therapeutic purposes [3].

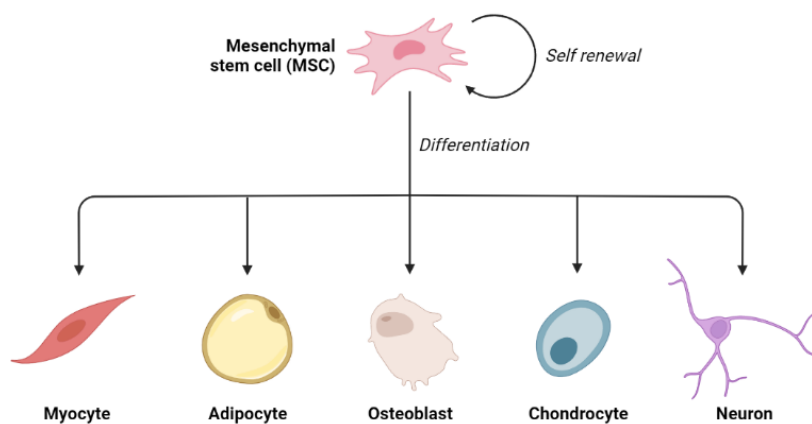


Figure 1. Schematic of MSCs And Their Ability to Self-Renew, Repair, and Differentiate Into Different Cell Types. MSCs are considered novel therapeutic agents and are studied for their repair and high-healing capability, and to better understand their ability to differentiate into a variety of cell types. Images created by BioRender, 2023.

Several engineering tools, such as dielectrophoresis coupled with microfluidic platforms, can be used for biomarker development in cell identification and characterization. Dielectrophoresis (DEP) is a novel cell analysis tool used to examine and manipulate biological cells. For instance, DEP can discern ABO blood groups [4] for rapid blood typing, discriminate between healthy and cancerous cells [5] for cancer detection, and purify subtypes of stem cells [6] to support stem cell therapies.

Additionally, DEP allows for label-free measurement of cells' electrophysical properties (membrane capacitance and cytoplasm conductivity) which may serve as numerical indicators of cell health and stem cell fate [6].

Motivation for Work

Many advances have been made in DEP; however, little is known about the role cell surface features play in DEP's governing principle, cell polarization. More specifically, the field of DEP defines the electrophysical properties as the cell's ability to store charge (membrane capacitance) and conduct an electrical current (cytoplasm conductivity) without making connections to the cell's biological function. This proposal's objective is to address this knowledge gap to

enable a deeper understanding of cell polarization and broaden the definitions of membrane capacitance and cytoplasm conductivity.

This work focuses on modifying the cell-specific glycosylation patterns that make up the glycocalyx using treatments of either Kifunensine (Kifu) or N-Acetylglucosamine (GlcNAc) to further develop membrane capacitance and cytoplasm conductivity as contenders for label-free biomarkers and determine the role of the glycocalyx on the polarization. We measured modifications made to the glycocalyx using DEP to investigate the contributions of the glycocalyx to membrane capacitance and cytoplasm conductivity in adipose tissue (AT) derived MSCs as a base model for comparison. A new parameter from DEP measurements, transient slope, was assessed as a third potential label-free biomarker. Modified and unmodified hMSCs were differentiated into adipocytes and osteocytes and verified through gene expression using qPCR analysis to see how glycocalyx modifications impact cell fate [6]–[8].

Specific Aims

Aim 1: Modify the Glycocalyx Using N-Acetylglucosamine (GlcNAc) and Quantify the DEP Response, Membrane Capacitance, Cytoplasm Conductivity, and Biological Function.

Aim 1 investigates the effect of modifying cell-specific glycosylation patterns that make up the glycocalyx using a 5-day treatment of GlcNAc. hMSCs treated with GlcNAc are expected to have an increase in multiple monosaccharide glucose to any exposed nitrogen-linked amines on the

glycocalyx, which increases a cell's overall area. The DEP response, membrane capacitance, cytoplasm conductivity, and biological function of hMSCs were measured.

Aim 2: Modify the Glycocalyx Using Kifunensine (Kifu) and Quantify the DEP Response, Membrane Capacitance, Cytoplasm Conductivity, and Biological Functions.

Aim 2 investigated the effect of inhibiting the glycosylation patterns that make up the glycocalyx using a 5-day treatment of Kifu. hMSCs treated with Kifu are expected to prevent the attachment of multiple monosaccharide glucose to the nitrogen-linked amino acid, which decreases the overall cell area. The DEP response, membrane capacitance, cytoplasm conductivity, and biological function were measured.

The studies completed in Aims 1 and 2 provide an understanding of the biological meaning of hMSCs' electrophysical properties. First hMSCs from adipose and osteocyte-derived stem cells were given a series of treatments to modify the glycocalyx to compare them to untreated cells in vitro. Then, baseline measurements of the electrical properties of untreated hMSCs were compared to the measured electrical signatures of treatment-modified cell populations. Additional experiments were conducted to determine how the electrical properties changed as hMSCs were treated, modified, and expanded in vitro. The electrical parameters of differentiating and non-differentiating treated and untreated hMSCs were collected to construct a correlation between the DEP

spectra and cell size and polarizability. Finally, the capability to sort hMSCs into their subpopulation based on their electrophysical properties (membrane capacitance and cytoplasm conductivity) was recorded. Those changes were then further verified using known gene markers to demonstrate that cells not only underwent differentiation but also the treatment and can be distinguished from one another. The changes observed were compared to their corresponding treatment and differentiation control as well as a double negative control (no treatment no differentiation).

The studies that were undergone during the experimental process only further help better understand how the biological function of stem cells can be further understood using DEP methods for distinguishing between heterogeneous subpopulations of stem cells. HMSCs have great therapeutic promise and the development of membrane capacitance and cytoplasm conductivity as label-free biomarkers positions DEP as supportive technology.

CHAPTER TWO: BACKGROUND

Heterogeneity of hMSCs

Heterogeneity in human mesenchymal stem cells (hMSCs) refers to the presence of diverse subpopulations within the cell population. In the paper from *Elahi, KC, et. al (2016)* noted that subpopulations exhibit variations in their characteristics, properties, and functionalities, due to factors like cell source, donor-specific differences [9], culture conditions, and passage number. *Elahi, KC, et. al. (2016)* and *Costa, Luis, et. al. (2021)* [9], [10] also explained hMSCs' heterogeneity is important for several reasons since different subpopulations possess distinct functional properties, affecting their ability to differentiate into specific cell types and secrete growth factors and cytokines [9], [10] necessary for their location.

Additionally, the therapeutic efficacy of hMSCs can be influenced by the presence of diverse subpopulations because certain subpopulations can display a high regenerative potential and immune-modulating properties. Another factor may be due to donor-specific heterogeneity in hMSCs, which impacts their quality, potency, and responsiveness in therapeutic applications [10].

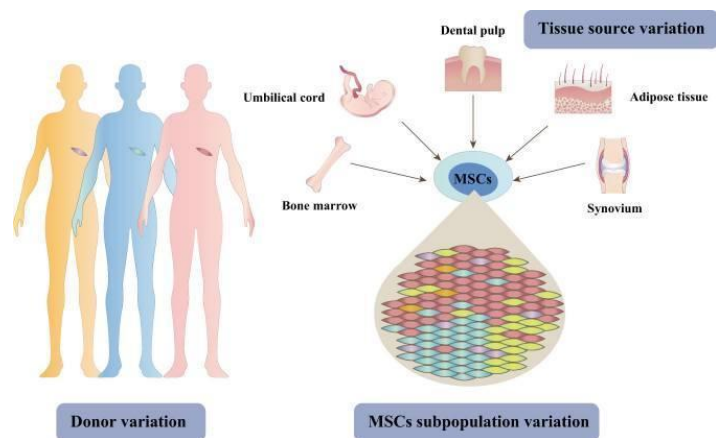


Figure 2. The Heterogeneity of MSCs (Adapted from *Zha, K et. al., 2021*) [11]. The image provides a representation of how MSCs can demonstrate implicit heterogeneity across a range of factors, including donors, tissues, and cell populations.

The function of MSCs can vary among different donors, as well as different derived tissue sourced. These variations manifest in differences in cellular properties displayed like cell proliferation, differentiation potential, and immunoregulatory abilities. Where even within the same tissue, MSCs are heterogeneous, with not all cells displaying identical cellular functions as described in *Zha, K et. al. (2021)* [11]. Specifically, hMSCs that are derived from diverse sources are not uniform and cannot be categorized by the expected tissue differentiation as previously explored by *Sacchetti, et al.'s (2016)* paper. Sacchetti's analysis concluded that cells are dependent on their origin and their "tissue-specific committed progenitors" determine how hMSCs respond to their new environment regardless of the differentiation they underwent [1] (Figure 3 below).

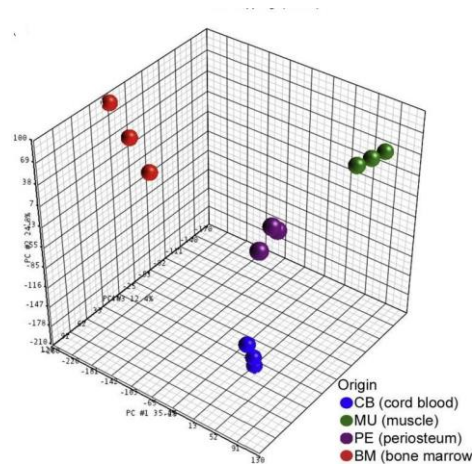


Figure 3. “Cell Surface and Transcriptomic Comparison of MSCs” from Different Tissues Types(Adapted from *Sacchetti, B et. al.’s 2016 paper*) [1]. Gene-expression profiling data of CD146+ cells from bone marrow (BM), cord blood (CB), muscle (MU), and placenta (PE) were subjected to unsupervised clustering analysis. The purpose was to explore if there were inherent groupings among samples based on correlations of gene-expression profiles. The results show how gene expression profiles and hierarchical clusters can produce distinct separations based on cell origin.

Understanding this heterogeneity is crucial for personalized medicine approaches. By recognizing and monitoring heterogeneity during in vitro expansion of hMSCs only those desired properties are maintained, and the loss of therapeutic potential is lessened. Heterogeneity investigation also aids in the discovery of biomarkers associated with desirable/unique properties or functional subpopulations, which can help equality control and enhancement [1], [10], [12]. Overall, comprehending, and characterizing heterogeneity in hMSCs is vital for selecting suitable subpopulations, optimizing culture conditions, and advancing regenerative medicine strategies.

What is Dielectrophoresis (DEP)?

DEP is a characterization technique that provides label-free electrophysical markers for cells [2], [5], [6], [13]. DEP employs a nonuniform electric field, created with electrodes, to induce cell movement based on the polarizability and inherent electrophysical properties (membrane capacitance and cytoplasm conductivity) of cells [14]. When the electric field is applied the field interacts with the ions available in the medium causing them to move and align around the cell (i.e., polarization) [13], which is directly impacted by the cell's biophysical properties.

The Clausius-Mossotti factor, also known as the Clausius-Mossotti equation or the Lorentz-Lorenz equation, is a parameter used to describe the polarizability of particles or molecules, including cells [4]. However, it should be noted that the Clausius-Mossotti factor is typically applied to describe the polarizability of homogeneous spherical particles rather than individual cells, which are more complex structures.

The Clausius-Mossotti factor (CMF) is given by the equation:

$$\text{CMF} = (\epsilon - \epsilon_0) / (\epsilon + 2\epsilon_0) \quad (1)$$

Where ϵ represents the complex relative permittivity (dielectric constant) of the material or medium surrounding the particles, and ϵ_0 is the permittivity of free space. The CMF correlates the polarizability of a particle to its dielectric properties and the dielectric properties of the surrounding medium. It also describes how the electric field interacts with the particle and induces a dipole

moment or polarization within the particle [4]. When observing cells, they are considered heterogeneous structures with complex shapes and compositions [10]. Their polarizability depends on a range of factors, like the distribution of intracellular and extracellular ions, membrane properties, cytoplasmic components, and cell overall cell area. These factors contribute to the overall dielectric properties and polarizability of the cell which are referred to in this paper as the electrophysical properties that make up the cell.

Although the CMF is not used to describe the polarizability of individual cells, it can be used as a theoretical framework for understanding the behavior of polarizable particles in cell suspensions or systems containing multiple particles. The CMF can help in describing the effective polarizability of cells or the response of the cell population to an external electric field.

Cells have distinct frequency-dependent polarizability that can be used for identification with DEP. Polarized cells will show either a positive DEP response (pDEP), wherein cells move to areas of high electric field strength, or a negative DEP response (nDEP), wherein cells move to areas of low electric field strength [6] (Figure 4). Thus, low, and high-frequency DEP measurements provide information about the cell membrane and cytoplasm, respectively.

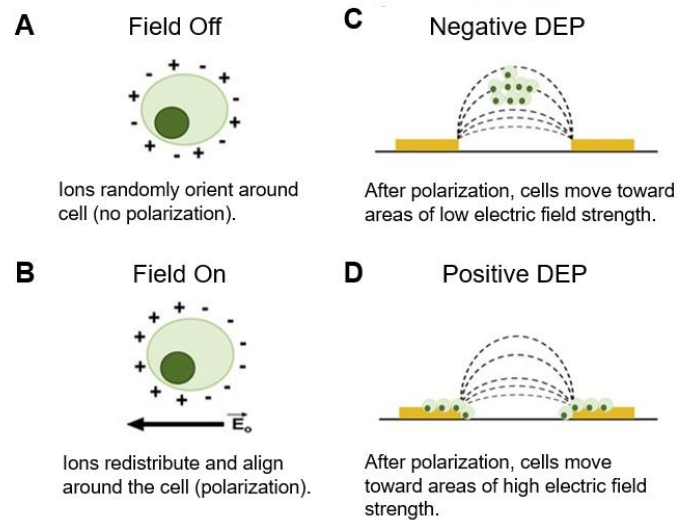


Figure 4. Schematic of How Cell Polarization and DEP Response Function in Cells (adapted from Adams, T.N.G., et al., 2018 [15]). The light green circle represents a cell, and the dark green circle represents the nucleus of a cell. 3A) the electrical field is off, ions randomly orient through the cell, with no polarization. 3B) When the electrical field is on, ions orient redistribute, and align around the cell, polarization. 3C) Cell movement is toward a low electrical field (dotted line), away from the electrode, negative DEP. 3D) Cell movement is towards a high electrical field (dotted line) towards the electrodes, positive DEP. The difference between positive and negative DEP responses depends on their movement [15].

Figure 5 is a visual representation of how pDEP and nDEP change according to the applied frequency. The electrophysical properties can be determined by using the DEP spectra to map the changes in polarity in cells. The cells' membrane conductance (yellow region), crossover frequency (zero-intercept), membrane capacitance (blue region), and cytoplasm conductivity (green region) occur over a region of zero to twenty Hz with the corresponding average DEP increasing logarithmic scale where DEP decreases as the frequency increases [4], [5], [7], [13], [16].

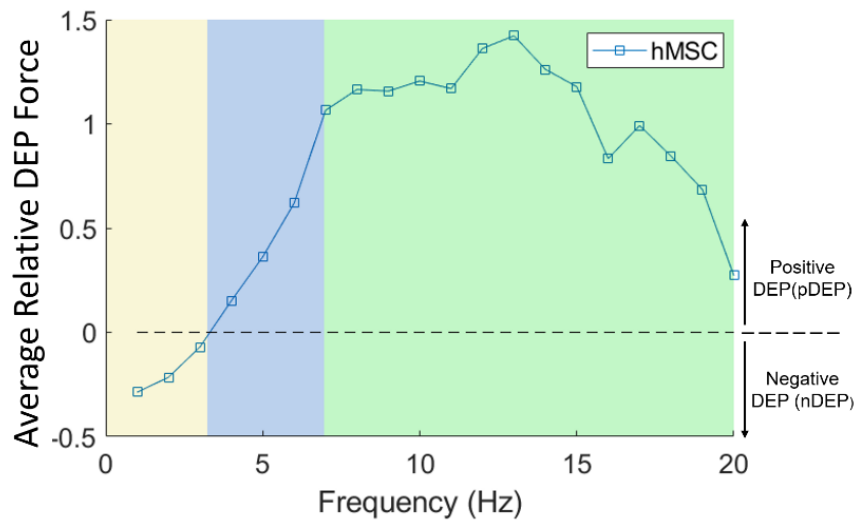


Figure 5. Visual Representation of The Positive and Negative DEP Responses Based On Changes In Frequency (adapted from *Tunglin, Tsai, et al, 2021 [4]*). The parts of the DEP spectra infer the cells' membrane capacitance (yellow region), crossover frequency (zero-intercept), membrane conductance (blue region), and cytoplasm conductivity (green region) [4].

Cell Polarization and DEP Spectra

Cell DEP polarization is characterized experimentally by measuring the pDEP and nDEP responses at specific frequencies. Visually, this means that at specific frequencies cells will appear along electrode edges for pDEP and not along electrode edges for nDEP, which is used to build a DEP response spectrum for each cell type (Figure 6). With heterogeneous populations of cells, both nDEP and pDEP cell behaviors are visualized at a single frequency. Using data points from the DEP response spectra the electrical properties of the cell membrane capacitance and cytoplasm conductivity are estimated.

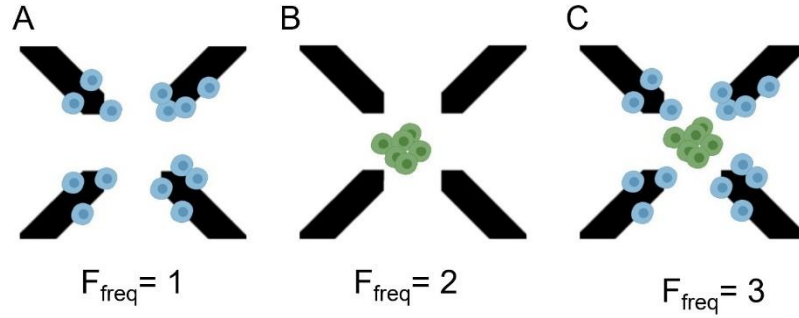


Figure 6. DEP Response Based on Frequency Changes (adapted from *Tunglin, Tsai, 2022*) [17]. The diagram is a visual representation of how DEP measurements where A, B, C are different frequencies. (A) represents a positive DEP, (B) a negative DEP response, and (C) a hypothetical DEP response for a heterogeneous cell population. The different frequencies demonstrated can help build DEP spectra for each cell type.

The membrane capacitance represents the ability of the cell membrane to store electrical charge. It can be estimated using the following equation:

$$C_{\text{mem}} = \epsilon_{\text{mem}} * A_{\text{mem}} / d_{\text{mem}} \quad (2)$$

where C_{mem} is the membrane capacitance, ϵ_{mem} is the relative permittivity of the membrane, A_{mem} is the surface area of the cell membrane, and d_{mem} is the thickness of the cell membrane. Cytoplasmic conductivity represents the ability of the cell cytoplasm to conduct electrical current. It can be estimated using the following equation:

$$\sigma_{\text{cyto}} = (G_{\text{mem}} * C_{\text{mem}}) / (G_{\text{mem}} + G_{\text{cyto}}) \quad (3)$$

where σ_{cyto} is the cytoplasmic conductivity, G_{mem} is the membrane conductance, C_{mem} is the membrane capacitance, and G_{cyto} is the cytoplasmic conductance.

The membrane conductance (G_{mem}) and cytoplasmic conductance (G_{cyto}) can be determined experimentally or estimated using appropriate models considering

the geometry and electrical properties of the cell [4]. It is also important to note that equations of membrane capacitance and cytoplasmic conductivity only provide an estimate. Both equations depend on the varying factors of each cell like cell type, experimental conditions, and cell state, and therefore used as a tool for quantifying parameters associated with DEP [4], [5], [10], [14].

Though membrane capacitance has been studied for hMSCs and other cell systems, specific molecular contributions to capacitance are unknown in the DEP field. Additionally, links between label-free measurements of membrane capacitance and hMSC function need exploration to provide insight for therapeutic purposes. Cells processed for DEP measurements experience a change in morphology. The more complex the cell surface the higher the membrane capacitance. Less complex surfaces or smooth cell membranes have an estimated capacitance of 9 mF/m^2 [14], [15]. One notable feature of the cell surface is the glycocalyx, a biointerface composed of glycolipids and glycoproteins that span across the cell membrane [4]. The glycocalyx contributes to the cell area, varying from 60 to 500 nm [4], [18], [19] in size. The size, molecular pattern (glycosylation), and content of the glycocalyx impact cell polarization and are detectable using DEP. In both neural stem and progenitor cells, glycosylation contributes to membrane capacitance, which is linked to the complexity of the cell surface which impacts the fate of neural stem and progenitor cells [20], [21].

Membrane capacitance has been illustrated as a feasible biomarker [5], [7], [22] and DEP as a potential sorting technology to reduce cell heterogeneity, however, it is not widely used for cell identification and selection. Gold standards include fluorescence- and magnetic-activated cell sorting (FACS and MACS), but both have biomarker limitations. Often the biomarkers used for FACS and MACS overlap between multiple cell types, making phenotypic analysis using surface biomarkers inadequate to define hMSCs. Consequently, there is a fundamental need to develop alternative biomarkers and sorting technology to reduce hMSCs heterogeneity via cell identification and selection. In the absence of such knowledge, realizing the full therapeutic potential of hMSCs for stem cell therapies will continue to be difficult [10].

The process of cell polarization involves the alignment of ions around the cell's surface. All cells have a glycocalyx, a biointerface composed of glycolipids and glycoproteins, as part of their cell surface [23]–[25]. This means when DEP cell polarization occurs ions are interacting with the glycocalyx and the contents of the glycocalyx may contribute to membrane capacitance and cytoplasm conductivity measurements. The primary focus will be on altering the glycocalyx of cells utilizing N-acetylglucosamine (GlcNAc) and Kifunensine (Kifu) to observe variations in DEP polarization and the electrophysical properties of hMSCs.

Glycocalyx of the Cell

The glycocalyx contributes to the complexity of the cell surface, impacts membrane capacitance, and potentially cell fate. The glycocalyx has cell-

adhesion molecules that enable cells to attach and guide the movement of cells. The cell's capacitor is made up of two conducting materials separated by an insulator, in cells, the extracellular and intracellular fluids are the conductors, and the lipid membrane is the insulator [21]. Since DEP involves cell polarization and the alignment of ions around the glycocalyx the cell's structural features as well as the size play a key role in changes that can be observed in the cell's electrophysical properties [2], [5], [16], [21], [22], [24], [26], [27].

Studies including DEP have proven that plasma membrane glycosylation affects membrane structure and surface area of a cell, which could affect whole cell membrane capacitance and behavior in DEP [3]. The glycosylation patterns change membrane microdomains associated with membrane infoldings, which lead to modifications in membrane surface area not detectable by phase contrast microscopy [5]. The cell surface glycocalyx depending on the function of the cell can have thickened membrane regions by increased structural attachments which can then affect capacitance, DEP responses, and cell area. The opposite is true for cells that have glycocalyx with fewer structural attachments [2], [14], [23], [24], [26], [28].

Figure 7 below is a depiction of glycocalyx complexity in a cell. The structure of the glycocalyx is entirely dependent on the type of cell, location, and function [2], [21], [24], [28], [29]. Each type of glycocalyx structure attached can be used for protection against something more complex like communication between cells and self-recognition [15], [21], [22], [24]. The overall complexity of

the glycocalyx is what can potentially give a better insight into how the cell area and DEP response can lead us to a better understanding of the biological function of a cell and potentially cell fate.

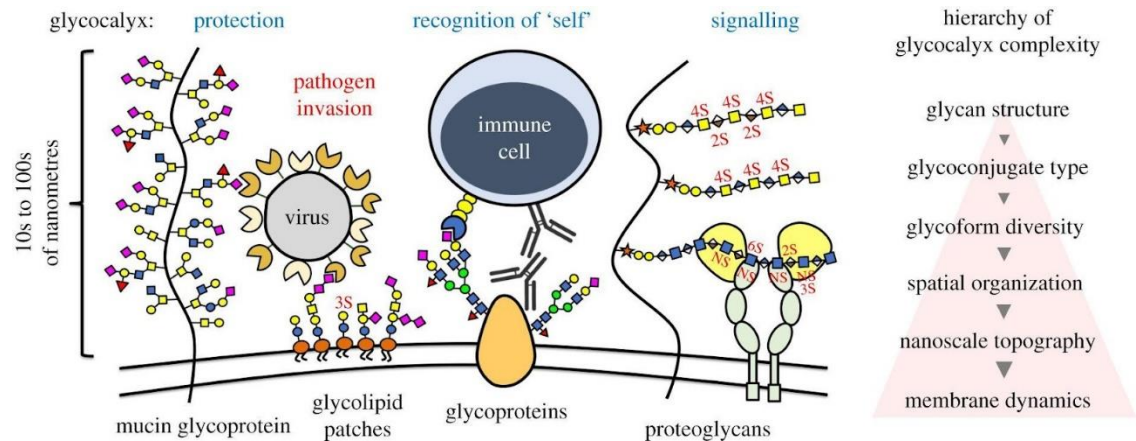


Figure 7. Representation of the Glycocalyx Complexity from (Purcell, S, et. al.,2019 [24]). The glycocalyx is depicted as the cell's biological interface facilitating the exchange of information between cells and their surroundings. The glycocalyx itself can vary in structure depending on what is attached, aiding in the diversity where structures attached allow the location-specific cells to function.

CHAPTER THREE:

MODIFYING THE GLYCOCALYX OF HUMAN MESENCHYMAL STEM CELLS

With the interest in characterizing and comprehending the heterogeneity of human mesenchymal stem cells (hMSCs) in the field of dielectrophoresis (DEP), this study focuses on investigating the DEP response and electrophysical properties of adipose tissue (AT) derived hMSCs through modification of the cell's glycocalyx. Human mesenchymal stem cells (hMSCs) are the model cell system explored because of pluripotent capabilities and heterogeneous populations in the interest of therapeutic medicines. AThMSCs were used throughout the experimental trial as a basis for understanding DEP response in relation to the cells' electrophysical properties and how it affect the biological function of the cells. Figure 8 represents the experimental workflow for the trials conducted.

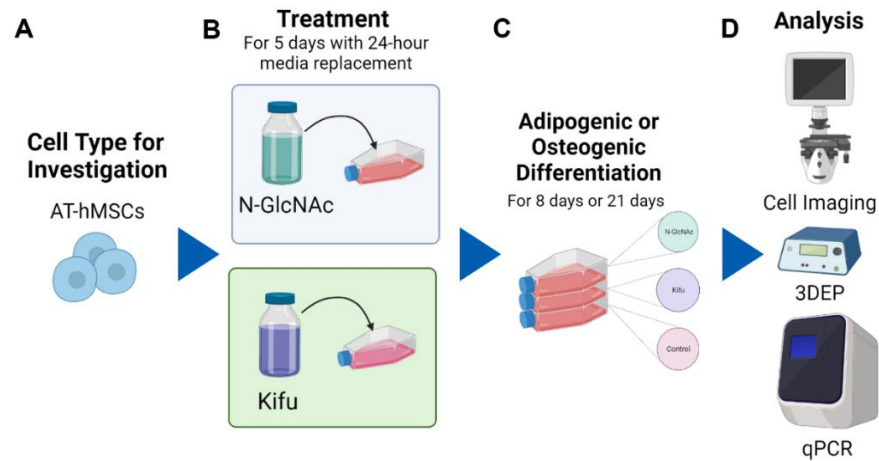


Figure 8. Experimental Workflow For (A) AT-hMSCs Glycocalyx Modification Using Treatment of Either GlcNAc or Kifu (B) with 24-Hour Media Replacement. All glycocalyx modification was monitored in vitro. Post-treatment cells continued to differentiate into either adipogenic (AD) or osteogenic (OS) for either 8 or 21 days. (D) Those differentiated cells were then analyzed under three methods. The cell's electrophysical properties were quantified first using the DEP response. The cell's biological function of cell fate was quantified using cell imaging for cell visualization during treatment and differentiation was coupled with qPCR. Control cells did not receive any treatment or were not differentiated but were treated in the same fashion as those undergoing treatment and differentiation. Image created by BioRender, 2023.

Since the membrane capacitance of a cell is proportional to the cell surface area, changes made in the glycocalyx can be detected using Kifunensine (Kifu) and N-acetylglucosamine (N-GlcNAc) [6], [15], [21], [29]. N-GlcNAc (shown in Figure 9) is an amine-derived monosaccharide glucose that adheres it through glycosylation to exposed nitrogen-linked amines [16], [18], [24], [26]. By using N-GlcNAc, more monosaccharide glucose is exposed to nitrogen-linked amines, which can increase the cell area (specifically the glycocalyx) therefore increasing the thickness.

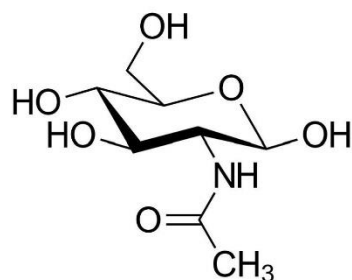


Figure 9. Molecular Structure of N-GlcNAc.

To decrease the glycocalyx thickness the cell surface will be modified using Kifunensine (Kifu). Kifu (shown in Figure 10) is an inhibitor for the mannosidase I enzyme that prevents glycosylation on the nitrogen-linked amino acid creating hybrid nitrogen glycans. These hybrid nitrogen glycans are linked to the amino acids that are stable in configuration inhibiting further the attachment of multiple monosaccharide glucose to the glycocalyx, therefore decreasing the overall cell area [30]. This modification can be measured using DEP by comparing modified hMSCs to unmodified hMSCs [4], [12], [22], [31].

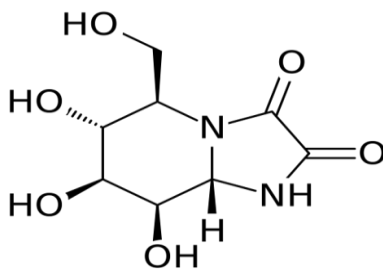


Figure 10. Molecular Structure of Kifu.

Materials and Methods

Cell Culture

AT-hMSC (ATCC, Manassas, VA) were cultured in MSC basal media supplemented with 2% FBS, 5 ng/mL FGF-1 (ATCC, Manassas, VA), 5 ng/mL FGF-2, 5 ng/mL EGF (ATCC, Manassas, VA), and 0.1X antibiotic-antimycotic. AT-hMSCs were grown in tissue culture-treated T-75 flasks coated with gelatin by seeding 5,000 cells/cm² and passaged at approximately 80% confluence.

Tissue culture-treated 6-well plates were coated with 0.2% gelatin in preparation for hMSC differentiation. For coating, lyophilized porcine skin gelatin (Sigma Aldrich, St. Louis, MO) was dissolved in Milli-Q water (MQ H₂O) and sterilized by autoclaving. 900 µL of the gelatin solution was added to each well in a 6-well plate and allowed to coat at room temperature for an hour using a lab bench rocker. The excess gelatin solution was aspirated, and the plates were placed in the biosafety cabinet to dry for at least 2 hours before plating. All AT-hMSCs regardless of the differentiation were imaged using an EVOS XL (Thermo Fisher Scientific, Frederick, MD) microscope at 4X to 40X objectives.

During cell passaging, the growth medium was aspirated, and the monolayer was rinsed once using 1X DPBS (Life Technologies, Carlsbad, CA). The cells were dissociated using 0.05% Trypsin-EDTA (ATCC, Manassas, VA) for 4 min at 37°C. When the majority of the cells were dissociated from the growth surface, residual trypsin activity was neutralized with an equal volume of trypsin neutralizer (ATCC, Manassas, VA). The removed cells were centrifuged

at 275 x g resuspended in the new growth medium and counted for accurate seeding and/or experimental processing.

HMSCs Differentiation

The AT-hMSCs used for differentiation were seeded at 10,000 cells/cm² in a gelatin-coated 6-well plate and were allowed to adhere/proliferate for 2 days before inducing differentiation. Care was taken to ensure the monolayer of differentiating cells was not disturbed during media changes.

For adipose differentiation, the growth media was aspirated and replaced with adipogenic medium, consisting of DMEM-HG (Thermo Fisher Scientific-Gibco, Frederick, MD) supplemented with 10% FBS (Corning Technology Center, Santa Barbara, CA), 50 mM of IBMX (MP Biomedicals, Irvine, CA), 1 mM of Dexamethasone (MP Biomedicals, Irvine, CA), and 0.1X antibiotic-antimycotic (Thermo Fisher Scientific-Gibco, Frederick, MD). The adipose differentiation media was changed every 2 days during the 8 or 21-day differentiation cycle. Particular care was taken to ensure the monolayer of the developing cells was not disturbed during media changes.

For osteocyte differentiation, the growth medium was aspirated and replaced with an osteogenic medium, consisting of α MEM (Life Technologies, Carlsbad, CA) supplemented with 10% FBS (Corning Technology Center, Santa Barbara, CA), 50 μ g/ml l-ascorbic acid 2-phosphate (FUJIFILM Wako, Richmond, VA), 100 nM dexamethasone (MP Biomedicals, Irvine, CA), 10 mM β -glycerophosphate (Alfa Aesar, Haverhill, MA), and 0.1X antibiotic-antimycotic

(Thermo Fisher Scientific-Gibco, Frederick, MD). Care was taken to make sure the monolayer of differentiating cells was not disturbed during media changes.

Reverse Transcriptase Quantitative Polymerase Chain Reaction (RT-qPCR)

RT-qPCR was used to quantify the gene expression changes during hMSC differentiation. RNA was extracted using an RNA micro prep kit (Zymo Research, Irvine, CA). The differentiation media was aspirated, and RNA was liberated from the monolayer by adding the lysis buffer and purified following the manufacturer's protocol. The cDNA was synthesized using LunaScript reverse transcription Master Mix (New England Biolabs, Ipswich, MA). Collagen type 1 alpha 1 (COL1A1), alkaline phosphatase (ALPL), and related transcription factor 2 (RUNX2) were used to quantify osteogenesis; and adiponectin (ADIPOQ), fatty acid binding protein 4 (FABP4), and peroxisome proliferator-activated receptor gamma (PPARG) were used to quantify adipogenesis [8]. Relative quantification of mRNA expression was obtained using the $\Delta\Delta C_t$ method using glyceraldehyde-3-phosphate dehydrogenase (GAPDH) as the endogenous control.

Treatment

AT-hMSCs underwent resuscitation and one initial passage at 80% confluency before conducting experimental trials to ensure cell population health and establish proliferation rate. All treatment media was prepared in the corresponding mesenchymal media needed for the cell type with all corresponding supplements for normal growth and treatment to meet the appropriate concentration. All cells regardless of treatment or differentiation were

incubated at 37°C and 5.0% CO₂ during the duration of the experiment before the analysis. After the first initial passage, cells were placed and prepped into their own individual T75 flasks at 5,000 cells/cm² and allowed to proliferate for 24 hours before the start of the treatment. Stock solutions of both GlcNAC and Kifu were created. The cells received a 100% media change every 24 hours for 5 days. After 5 days of treatment cells were differentiated into adipocytes or osteocytes for 8 or 21 days. The controls throughout the experiment did not receive treatment or differentiation by being treated under the same conditions as those cells that were treated and differentiated. Throughout the experimental trial, cells were imaged for visualization.

Histological Staining

Differentiated and treated hMSCs were fixed with 4% paraformaldehyde for 15 min at room temperature. After 15 min the hMSCs were rinsed three times with 1X DPBS and stored in 0.05% Sodium Azide in 1x PBS at 4°C. To assess osteocyte differentiation Alizarin Red S (ARS) was used to stain the calcium deposits. An ARS stock solution was made by dissolving 40mM ARS in Milli-Q water and sterile-filtered. HMSCs were incubated in ARS for 15 min at room temperature. The ARS was aspirated, and the cells were rinsed with Milli-Q water until any unbound ARS was washed away.

To assess adipocyte differentiation Oil Red O (ORO) was used to stain lipid accumulation. The ORO stock solution was prepared by mixing 0.5% (w/v) ORO dissolved in pure isopropanol with Milli-Q water at a 3:2 ratio. Before use,

the solution was left untouched for 20 min where after the allotted time was sterile filtered. The hMSCs were incubated in ORO for 10 min at room temperature and then aspirated while rinsing the cells three times with Milli-Q water. All cell samples were imaged immediately after staining using EVOS XL (Thermo Fisher Scientific, Frederick, MD). Histological method derived from reference [17].

Results and Discussion

GlcNAc and Kifu Treatments

GlcNAc and Kifu treatments were made to explore the basic principles of DEP cell polarization and expand our definition of electrophysical properties. Before treatments, the samples of cells were cultured at the same concentration (7.5×10^5 cells/mL) in an incubator at 37°C and 5.0% CO₂. Media was replaced every 24 hours to ensure an adequate amount of GlcNAc or Kifu was present throughout the 5 days of treatment. These media replacements account for the heat degradation of GlcNAc and Kifu in the incubator and increase the probability that a modification occurred. Daily cell images using an EVOS microscope at 40x magnification. All images were adjusted to grayscale with 20% contrast/brightness optimization for better visualization. Figure 11 displays images of one experiment of hMSCs treated with GlcNAc and Kifu. For the control, no treatment was administered and was overseen in the same fashion as treated cells with 24-hour proliferation media changes. Comparisons between the Kifu-treated cells and the control demonstrate a similar proliferation rate

throughout. GlcNAc-treated cells had a higher proliferation rate when compared to the control, especially at day 3 with a visible increase in the number of cells. In addition to differences in proliferation rates, cells' monolayer growth was also different. Cells that underwent GlcNAc treatment appeared opaque, making it easier to image, while cells treated with Kifu appeared translucent making imaging more difficult. In other words, cells modified with GlcNAc have more external monosaccharide glucose, and greater cellular area and therefore are opaquer than cells modified to have less external monosaccharide glucose attachments and less cell area (Kifu treatment).

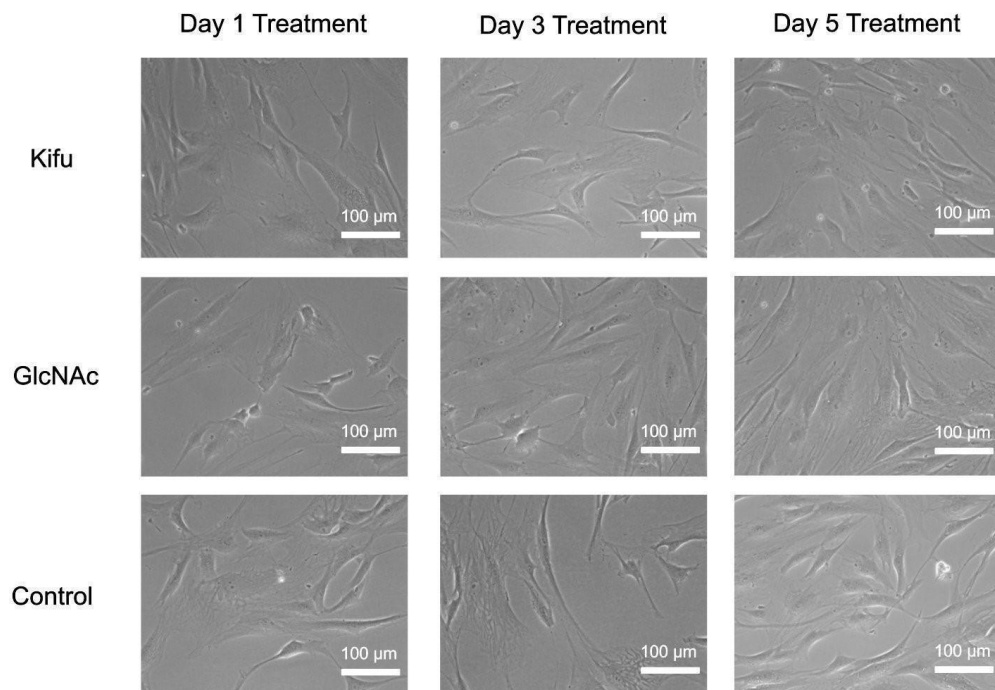


Figure 11. EVOS XL (Thermo Fisher Scientific, Frederick, MD) Microscope Images (40x Magnification) of AT-hMSCs that Underwent 5-Day Treatment of GlcNAc or Kifu. Images on Days 1, 3, and 5 are shown as a representation of visible changes observed during the 5-day treatment. Before treatments, the

samples of cells were cultured at the same concentration (7.5×10^5 cells/mL) in an incubator at 37°C and 5.0% CO₂. Replacement of media occurred every 24 hours to ensure an adequate amount of GlcNAc or Kifu was present on all 5 days of treatment. On an important note, the control cells were overseen the same as treated cells with a proliferation media change every 24 hours. The Kifu-treated cells and the control had similar proliferation rates. The GlcNAc-treated cells had the highest proliferation rate.

Cell Differentiation Post- GlcNAc and Kifu Treatments

The results were based on the treatments of GlcNAc and Kifu treatments that changed the morphology and electrophysical properties (DEP response) of the treated compared to the control. At the time of the experimentation period, it was important to determine if changes due to differentiation in the same treated cells impact the DEP response and its additional analysis perimeter for review. Cells underwent 8 days of differentiation after treatment (of 5 days), where the control cells were treated in the same fashion as those undergoing differentiation. All cells regardless of treatments were compared to the control as a baseline for changes recorded and observed. Differentiated cells were compared to the corresponding treatment control to determine if the changes recorded could be observed. Figure 11 above is a representation of one experimental trial of the data collected for treatments conducted. Overall, the treatment and differentiation of the cells result in a visual representation of the DEP response differences.

DEP Response and Glycocalyx Modification

Since DEP involves the alignment of ions around a cell's surface and the complexity of the cell surface is important, DEP measurements for the GlcNAc and Kifu treatments. After differentiation, cells were either processed for DEP or

RT-qPCR analysis. For DEP analysis the method described in reference [17] was used to prime and test all samples. The chip with cell sample was run on the 3DEP analyzer using 20 log-linear frequencies ranging from 2 kHz to 20 MHz at 10 Vpp for 60 seconds. The DEP response was evaluated using the 3DEP analyzer software and individual runs with an R-value > 0.9 were used in further analysis (approximately 10 runs for each experiment). All experiments were imaged on a hemacytometer where ImageJ software was used to determine cell size distribution [17].

The conductivity of buffer solutions and manual cell counts were done before DEP characterization using the 3DEP analyzer (LabTech, 224 East Sussex, UK). Figure 12 provides hypothetical representations of change to the cell's surface with GlcNAc and Kifu treatments. The more (or less) glucose on the cell surface will impact the alignment of ions for polarization.

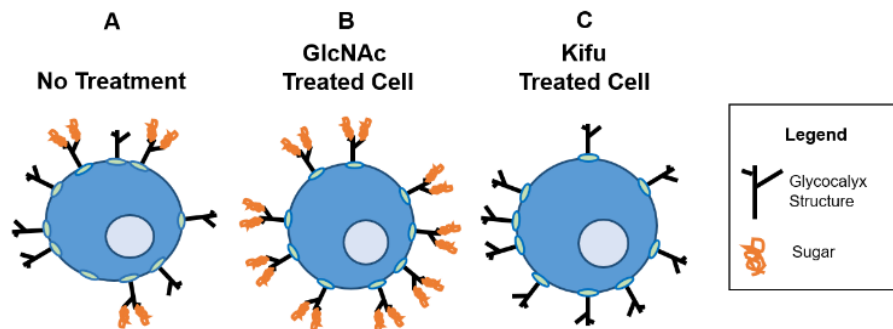


Figure 12. Schematic of the Cell Surface with (A) No Treatment, (B) GlcNAc Treatment, and (C) Kifu Treatment. A cell that has not undergone treatment will have a baseline number of sugars on the surface adapted from *Flanagan, L., et al. (2008)* [22]. The GlcNAc treatment increases the amount of sugar on the surface (more orange structures) and the Kifu treatment decreases the amount of sugar on the surface (fewer orange structures). These differences in the cell

surface (i.e., cell surface complexity) will influence DEP cell polarization and the resulting DEP spectrum. In turn, the electrophysical properties estimated from the DEP response/spectrum help make connections between the electrophysical properties of the cell and the biological function.

Histological Staining Post GlcNAc and Kifu Treatments

To further prove a modification of the glycocalyx, AT-hMSCs with the same passage number as those that underwent other analysis perimeters differentiated for a total of 8 or 21 days after treatment. AT-hMSC cells that were used for histological staining underwent differentiation into either adipocyte or osteocyte cells. All differentiated cells are compared not only to the corresponding differentiated control but also to a double negative control that has not undergone treatment or differentiation. Controls for the treatment type are also used as a comparison of differentiation between treatments where treated controls have only undergone treatment but no differentiation. All cell samples were immediately imaged after staining using an EVOS XL (Thermo Fisher Scientific, Frederick, MD) microscope. Figure 13 and Figure 14 show 20X magnification images with a 20% brightness adjustment for better visualization.

To assess adipocyte differentiation, Oil Red O (ORO) stains target lipid accumulation in the sample cells. Cells that have visually more "red" pigmentation in the cell's images lead to higher concentrations of lipid cells. Sample cells used osteocyte differentiation Alizarin Red S (ARS) to assess the calcium deposits. Cells that have visually more stained/noticeable "dark red" edges of sacs are regarded as having a high concentration of calcium cells.

Histological Stains and Glycocalyx Modification

All images compared to the differentiation control (Figures 13 and 14; 3A and 3B for Day 8 differentiation and 6A and 6B for Day 21 differentiation), the double negative control (Figures 13 and 14; 3C for Day 8 differentiation and 6C for Day 21 differentiation) and treated control (Figure 13 and 14; 1C, 2C for Day 8 Differentiation and 4C, 5C for Day 21 differentiation). Both Figures 13 and 14 demonstrate that Day 21 is a better representation for understanding how treated (GlcNAc or Kifu) and differentiated (adipogenic or osteogenic) cells differ visually. This suggests that although Day 21 is better for determining the differentiation for those GlcNAc or Kifu treated cells, cells modified and differentiated tend to differentiate better if the parent cells originally derived from the same tissue cell are the same type of differentiated cell. Sample cells originally derived from adipose tissue and therefore have a higher propensity to become adipose tissue. The opposite is true if the differentiated cells are different from the originally derived cells making it difficult for the cells to become another cell type.

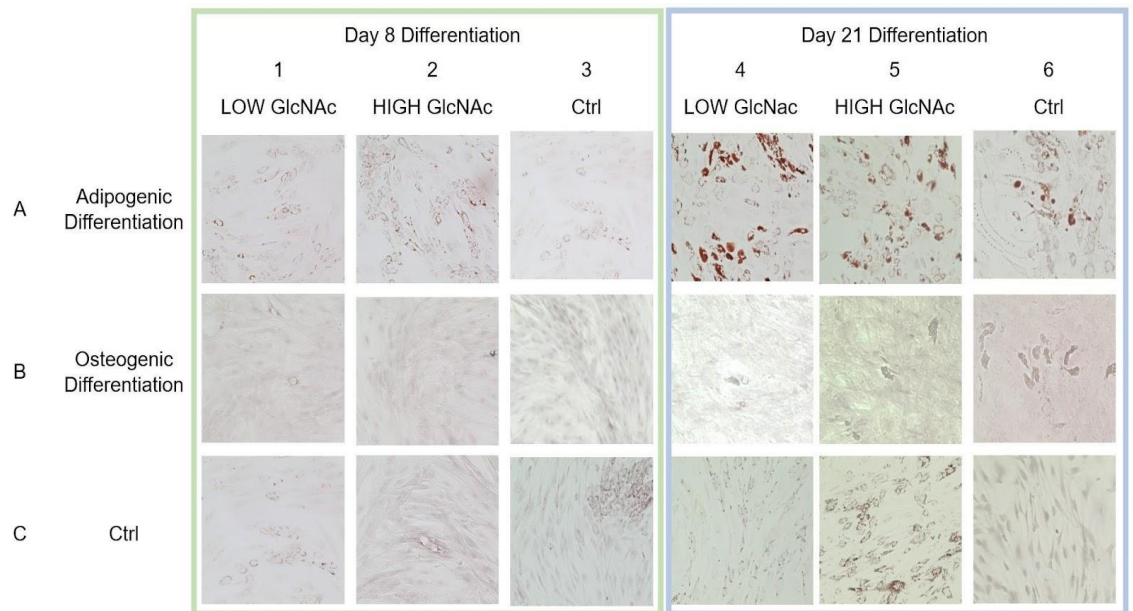


Figure 13. Keyence Microscope Images (20x Magnification) of AT-hMSCs that Underwent 5-Day Treatment of GlcNAc and then an 8-Day or 21-Day Differentiation. Images on Day 8 and Day 21 of differentiation are shown as a representation of visible histological changes observed during the differentiation process. The treated cell samples are differentiated in an incubator at 37°C and 5.0% CO₂ where the media is replaced every 2 days until the differentiation time is complete. On an important note, the differentiated control cells (3A, 3B, 6A, and 6B), treatment control cells (1C, 2C, 4C, and 5C), and the double negative control cells (3C and 6C) overseen in the same fashion as the treated differentiated cells with a proliferation media change every 2 days.

Based on Figure 14 below, Day 8 sample cells demonstrated little to no differentiation observed when comparing Day 8 GlcNAc treated and differentiated cells to the Day 8 controls. At Day 21 differentiation both high and low GlcNAc treated cells had a high adipose production when compared to the differentiated control, treated control, and double negative control. When comparing osteogenic differentiation in Figure 14, both low and high-GlcNAc-

treated cells show little to no differentiation when observing the differentiation control and the double negative control.

Overall, GlcNAC-treated cells (both high and low) differentiate visually similar to adipogenic control whereas the treatment control cells appear to be significantly different than the double negative control. Osteogenic differentiation of the treatment cells is negligible in the amount of calcium stained when compared to the osteogenic control. The Day 21 differentiation data does visually prove that modifications made using the GlcNAC treatment as both treatment controls differ from the double negative control (3C) and both treatments of GlcNac successfully differentiated into a specific cell type when compared to the differentiated control and the double negative control.

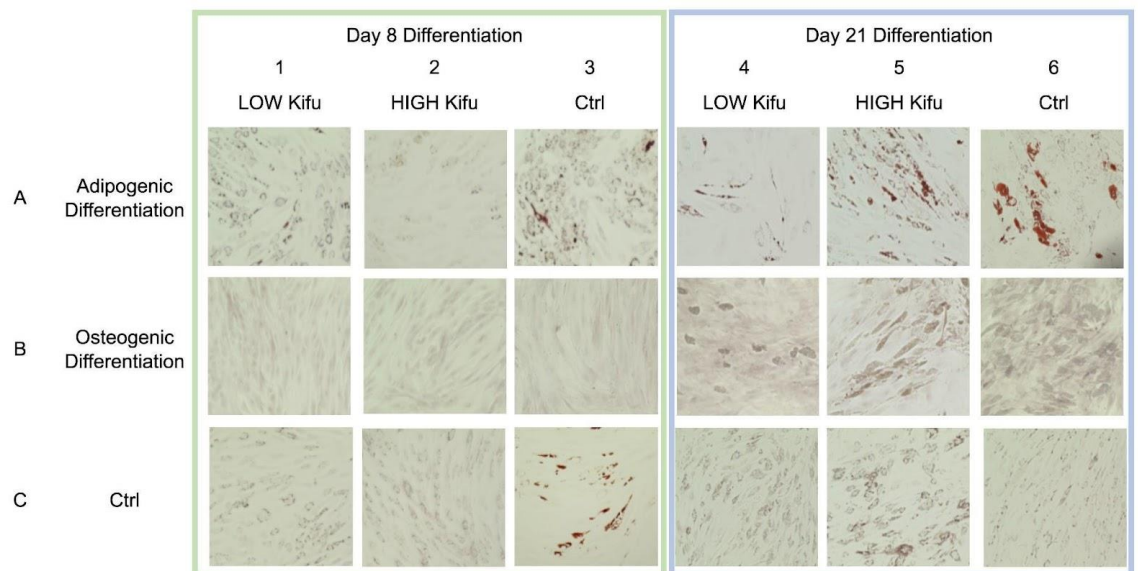


Figure 14. EVOS XL (Thermo Fisher Scientific, Frederick, MD) Microscope Images (20x Magnification) of AT-hMSCs that Underwent 5-Day Treatment of Kifu and then an 8-Day or 21-Day Differentiation. Images on Day 8 and Day 21 of

differentiation are shown as a representation of visible histological changes observed during the differentiation process. The treated cell samples are differentiated in an incubator at 37°C and 5.0% CO₂ where the media is replaced every 2 days until the differentiation time is complete. On an important note, the differentiated control cells (3A, 3B, 6A, and 6B), treatment control cells (1C, 2C, 4C, and 5C), and the double negative control cells (3C and 6C) overseen in the same fashion as the treated differentiated cells with a proliferation media change every 2 days.

DEP Characterization

Figure 15 shows the DEP spectra for each treatment, treatment with differentiation, and control along with estimated electrophysical properties. In Figure 15A, the average DEP spectrum of the GlcNAc-treated cells is like the average DEP spectrum of the control. This suggests that the GlcNAc treatment had little to no impact on the glycocalyx of the cells. However, there is a visible difference between the average DEP spectrum of the Kifu-treated cells and the control. More specifically, the spectrum of the Kifu-treated cells has a higher relative DEP force and crosses the zero line at unique frequencies. This suggests that the Kifu treatment modified the cell's glycocalyx and electrophysical properties. When looking at only the GlcNAc-treated cells with differentiation, Figure 15B, there are visible differences between the average DEP spectrum of the GlcNAc-treated cells with adipocyte differentiation (AD, blue curve), the GlcNAc-treated cells with osteoblast differentiation (OS, gray curve), and control. Yet, when looking at the Kifu-treated cells with differentiation, Figure 15C, there are more pronounced differences in the average DEP spectrum of the Kifu-treated cells with AD (yellow curve), Kifu-treated cells with

OS (green curve), Kifu treatment no differentiation (light blue curve), and the control. Interestingly, the GlcNAc treatment with OS increases the relative DEP force experienced by the cells and Kifu treatment with OS decreases the relative DEP force experienced by the cells [4]. This data illustrates that differentiation changes the cell in a manner discernible with DEP measurements. The most notable differences are comparing Kifu-treated cells to their control. Kifu-treated cells had significant differences in the DEP spectra creating distinct lines between the types of Kifu cells (as observed in Figure 15C).

Figure 15D combines all the average DEP spectra and 15E summarizes the cell size, cytoplasm conductivity, membrane capacitance, and the maximum relative DEP force. The size of the cells varied with treatment and differentiation. The GlcNAc and Kifu treatments increased cell size, GlcNAc with differentiation increased cell size, and Kifu with differentiation decreased cell size. The cytoplasm conductivity varies with treatments and differentiation and corresponds to the differences observed at higher frequencies in Figure 15D. Interestingly, membrane capacitance is similar for all treatment conditions except Kifu AD. The maximum relative DEP force varies for all treatment conditions. The data in Figure 15 demonstrates that Kifu-treated cells with and without differentiation yield the largest change in the cells reflected in their size, cytoplasm conductivity, membrane capacitance, and maximum relative DEP force. This supports literary evidence that membrane capacitance is proportional to the cell's surface area [5],

[6], [8]. It is also worth noting that buffer conductivity for this experimental trial had an average measurement of 103.6 $\mu\text{S}/\text{cm}$.

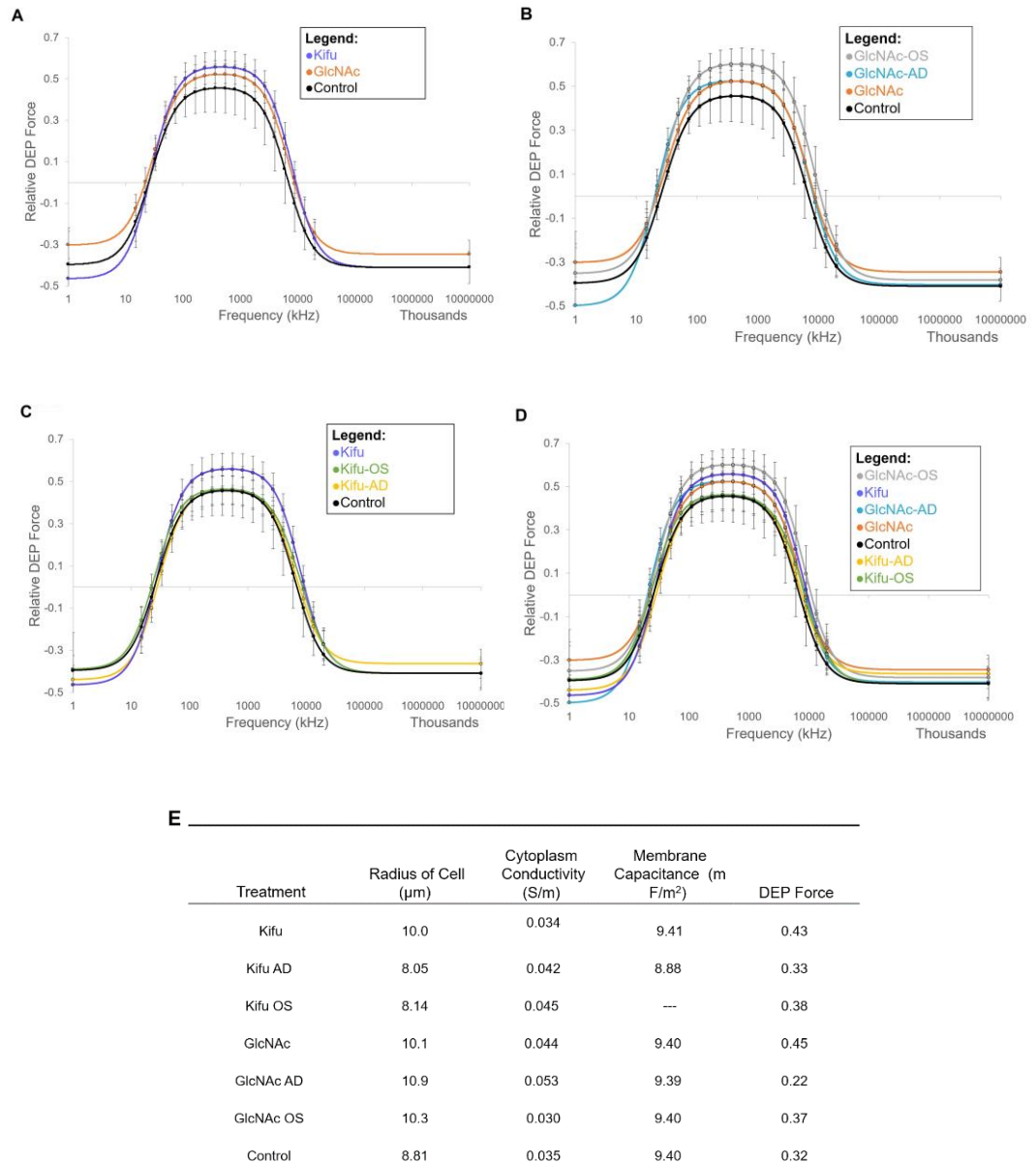


Figure 15. DEP Response of AT-hMSCs with (A) GlcNAc and Kifu Treatments, (B) GlcNAc Treatment with Adipocyte Differentiation (AD) and Osteoblast Differentiation (OD), (C) Kifu Treatment with AD and OS, and (D) Combination of All Treatment Conditions. (E) Provides Cell Size and Estimations of Cytoplasm

Conductivity, Membrane Capacitance, and the Maximum Relative DEP Force. .
The largest differences in cells we observed in Kifu treatments coupled with differentiation follow with values reported in E.

CHAPTER FOUR: CONCLUSION

Determining stem cell heterogeneity and understanding its role in biological function is a fundamental aspect of cell biology. The heterogeneity of stem cell samples can provide valuable insights into its structure (i.e., the glycocalyx), organization, and physiological properties. One technique that has proven effective in determining cell heterogeneity based on their electrical properties is dielectrophoresis (DEP). DEP is a powerful tool that utilizes the electric field to measure and analyze the electric properties of cells. By subjecting cells to an electric field, DEP can evaluate the response of cells based on their size, shape, and membrane properties. As cell samples vary in heterogeneity, DEP can help determine the amount of heterogeneity by measuring the membrane capacitance and cytoplasm conductivity of cells. The electrical properties of a cell are influenced by its size, as larger cells have a larger surface area and different membrane characteristics compared to smaller cells. We define heterogeneity or the amount of heterogeneity based on the number of different cell types present in a stem cell sample.

DEP can provide valuable insights into the overall biological function of cells. By analyzing the electrical signatures of cells, researchers can assess their physiological state and functional properties. For example, DEP has been used to investigate the differentiation potential of human mesenchymal stem cells (hMSCs) into various tissue types, such as adipocytes and osteoblasts. In my

work, the modification of glycocalyx treatments have been successful when looking at the cells visually. However, proof of glycocalyx modification is more notable in the DEP response spectra of the cells. Those cells that underwent treatment when compared to their respective control had a separate DEP response. Even treated cells when compared to one another have different DEP response spectra making the argument that DEP not only can help reduce heterogeneity in cells, but it can visually show those changes using the DEP spectra. Although DEP provided more information regarding the difference in cells when treated it is still unclear how those modifications affected the biological function of the cells and what genes were expressed after treatment and differentiation compared to those cells that were only treated. The label electrical biomarkers (membrane capacitance and cytoplasm conductivity) obtained through DEP analysis can be correlated with the differentiation profile of hMSCs, providing quantitative data on their differentiation potential.

DEP can be utilized to explore and optimize additional bioassays to further understand the biological function of cells. For instance, quantitative differentiation assays can be developed to establish a stronger correlation between the electrical biomarkers obtained through DEP and the differentiation potential of hMSCs into various cell lineages, such as cartilage tissue, cardiomyocytes, or hepatocytes.

Additionally, cytokine and growth factor secretion assays can be designed to investigate the relationship between the electrical biomarkers and the

paracrine and immunomodulatory properties of hMSCs. These assays can shed light on the potential therapeutic applications of hMSCs in tissue regeneration and immunotherapy.

As future work, DEP can be used to aid in the characterization of sorted subpopulations of cells. By using DEP to sort hMSCs (i.e., manipulate their heterogeneity) into distinct groups based on their electrical properties, researchers can verify the successful separation of cells with different electrical biomarkers. The sorted subpopulations can then be further characterized using DEP to examine their electrical properties and compare them to the unsorted population. This analysis can provide insights into the differences in electrical signatures and biological activities between the sorted and unsorted cells. The sorted subpopulations can be expanded and subjected to differentiation assays to investigate their differentiation potential into adipocytes and osteoblasts, by the correlations observed in previous studies. The growth characteristics of the sorted subpopulations can be monitored and compared to the bulk measurements obtained from the unsorted population, providing a comprehensive understanding of the impact of electrical biomarkers on cellular behavior during expansion and differentiation processes.

APPENDIX A:
POSTER PRESENTATION DISPLAYS

Below is a summary of the three conferences where the research conducted on modifying the glycocalyx of hMSCS was displayed and shared with other scientists and the public. Figure A1 below is one representative poster.



Figure A.1. Preceding Poster Presentation, 2022. All Data Represented and Displayed was Preliminary.

1. California Institute of Regenerative Medicine (CIRM) Bridges Conference
2022 | San Diego, CA

The CIRM Bridges program provides paid regenerative medicine and stem cell research internships to students at universities and colleges that do not have major stem cell research programs. Each Bridges internship includes thorough hands-on training and education in regenerative medicine and stem cell research. Every year CIRM hosts the “CIRM Bridges Conference” for the CIRM Bridges scholars (those who were awarded the scholarship for the CIRM Bridges program) to present the research they studied and how their studies can improve medicinal sciences. Students across all the colleges and universities in California who received the scholarship come to present their works and help support the reason for CIRM’s mission to increase areas of research in fields of regenerative and stem cells to help nurture innovative ideas and potential solutions to illness and disease.

2. Inland Empire Stem Cell Consortium Symposium (IESCCS) 2022 |
California State University, San Bernardino

IESCC is a collaborative group of researchers from universities that include the University of California, Riverside, Western University of Health Sciences, Loma Linda University, and California State University, San Bernardino. The Consortium aims to encourage a

collaborative environment for stem cell research in the Inland Empire region. Its goals include promoting interaction among stem cell laboratories, offering training opportunities in stem cell biology for students, and raising awareness about stem cell research within the local community. To ensure its mission, the IESCC organizes joint activities such as seminar series, outreach programs, and an annual symposium.

3. Open House | University of California, Irvine - Dr. Tayloria Adam's Lab
The Open House event hosted at the University of California, Irvine (UCI) as a collaboration between the researchers in the Department of Chemical and Biomolecular Engineering at UCI as an outreach program for elementary age students to learn about potential careers or research they can do while in a university setting. The Open House event was also geared to highlight each laboratory's specialty and their research on stem cells. This event not only catered to other research colleagues through the campus but also invited potential investors to help contribute to stem cell research and the importance of science.

APPENDIX B:
CO-CULTURING HUMAN MESENCHYMAL STEM CELLS

Co-Culturing Cells

Cell culturing is an important technical process that allows scientists to better understand how cells adapt, grow, and are maintained under a controlled laboratory environment. The culturing of cells not only plays a role in understanding cells but also in the discovery of new treatments and knowledge of cellular functions.

The cells used throughout the experimental process were human mesenchymal stem cells (hMSCs) that were derived from either adipose, osteocyte, or umbilical cord tissue. This adaptation for co-culturing two cell lines can grow together under the same circumstances was largely done as a side-project to determine what the DEP response for co-cultured cells displayed and to see if two cell lines can co-exist rather than influence (in terms of growth) another cell line. The use of data was primarily for informational purposes and to determine whether co-cultures can be used as an alternative to tissue repair or regenerative medicine.

APPENDIX C:
HUMAN MESENCHYMAL STEM CELL SORTING USING A CYTOCHIP

The CytoRecovery’s ‘Cytochip’ is a microfluidic-based device, which uses the principles of hydrodynamic manipulation, induced electricity for sorting of cells or live/dead assessments of human mesenchymal stem cells (hMSCs). The Cytochip utilizes 3D small-scale pillars and channels and continuous fluid control to manipulate cells and achieve high-throughput analysis or sorting.

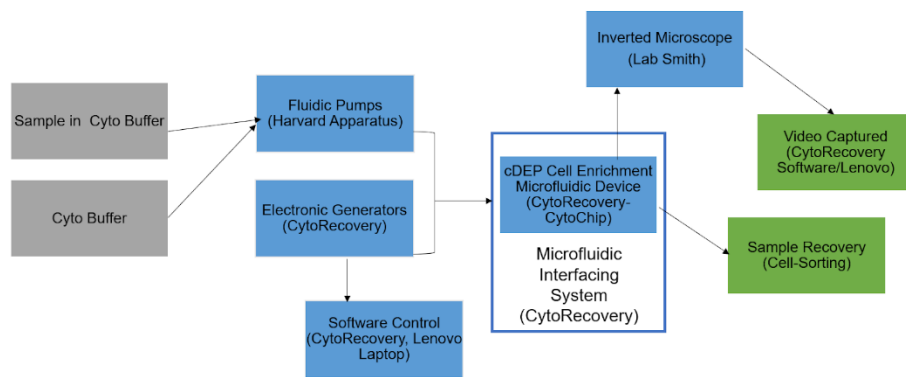


Figure C.1. Schematic overview of the CytoRecovery’s workflow used in this experiment. The core technology employs contactless dielectrophoresis (cDEP) microfluidic device, where the cells are suspended in proprietary Cyto Buffer provided by the company CytoRecovery, then a series of pumps and generators create a constant flow rate and energy input for the cells to pass through the Cytochip. Once the desired flow rate and energy have trapped your specified cells the untrapped cells are collected. The apparatus setup allows for video recording of all cell-sorting experiments [32].

Figure C.2 (below) is a representation of CytoRecovery’s Cytochip created for cell sorting. The device contains two inlets that allow for attachment of cells suspended in CytoBuffer and another for CytoBuffer pressure maintenance. Both inlets are controlled by flow rates provided by the Harvard pumps. Once the parameters are set the generator is set to a desired interest and cells and buffer

are pushed throughout the apparatus. Because the generator creates an electric field those cells targeted will either be trapped if there is an attraction/polarity to the cells or untrapped continuing to flow through and collected via the outlet.

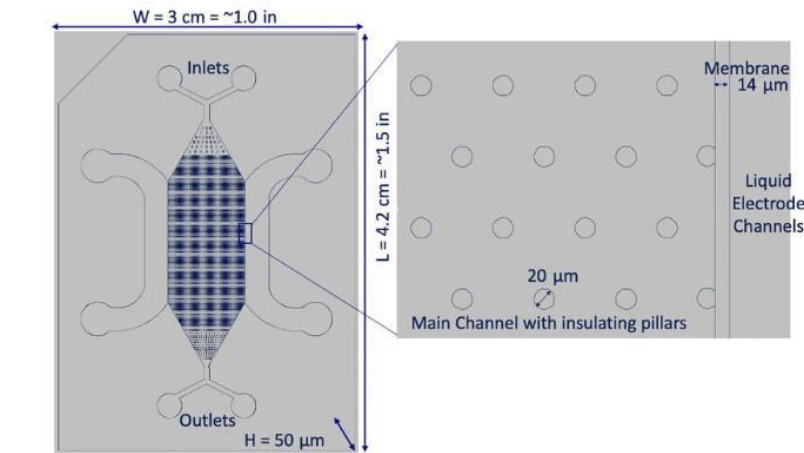


Figure C.2. Schematic of the CytoChip provided by CytoRecovery interfaced with electronics and fluidics systems for the cell sorting experiment. Image rendering provided by Hyler, A. (2021) [32]. Cells sorted were visualized using an inverted microscope with laptop-based software control. The cDEP device is constructed in a single layer out of COC containing 20 μm pillars and a 14 μm membrane that allows electrical fields to pass but retains separation of the sample and the liquid electrodes (cDEP) [32].

All samples during cell-sorting testing phase were cultured to approximately 80% confluency with an approximate cell count of 2.3 million cells dedicated to cell-sorting. After cells were sorted, they were plated into corresponding wells to ensure overall health and proliferations rates were not disturbed. If the test cells were viable, then the next process was to assess for differentiation after cell-sorting. Therefore, the cells would have to undergo 24hours in normal media for ensured adhesion and then be switched to

differentiation media. Figure C.3 is a representative image of the DU-145 cells (prostate cancer cells) that were sorted and plated after sorting experimentation was complete.

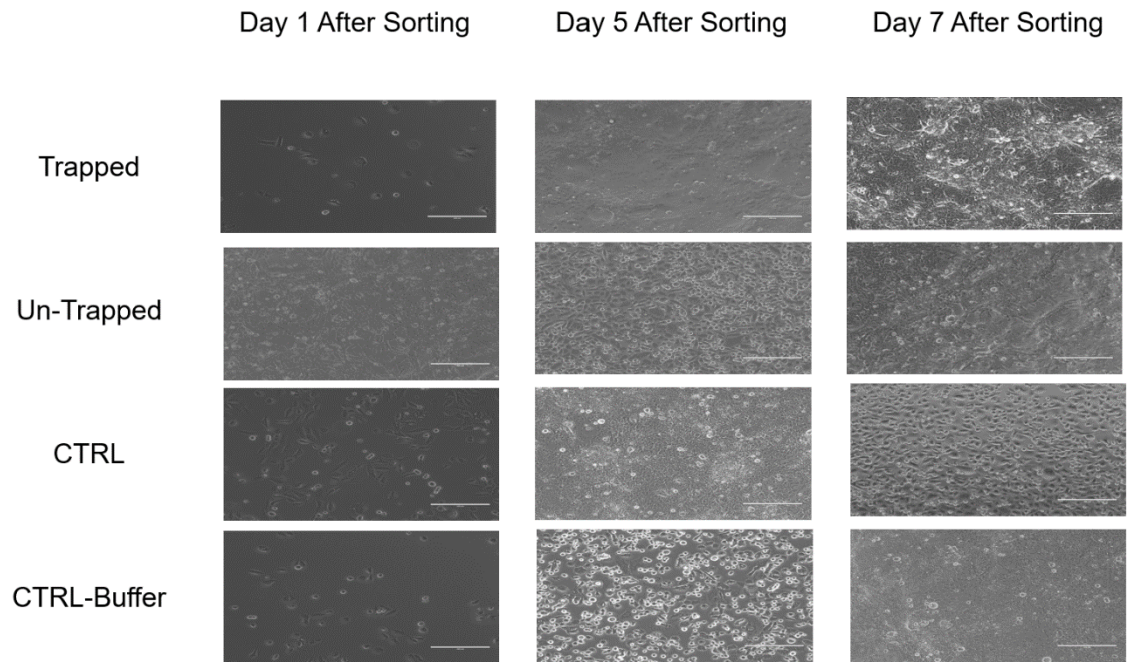


Figure C.3. Representative sample of a cell sorting experiment conducted using DU-145 cells. Cells collected underwent a 2-hour sorting experimentation at 200KHz with 46 gain as set parameters. It is important to note that the cells were prepped after reaching approximately 80% confluency and were harvested at a 2.3 million cell/mL concentration for the sorting experiment to have the necessary flow rate and time to sort.

Figure C.3 demonstrated that there are fewer number of trapped cells sorted under the parameters selected compared to the control. Trapped cells are referred to the cells under set parameters adhered/were attracted to the CytoChip because of the polarity experienced during the sorting process. The

control in this case did not undergo cell sorting, whereas the control-buffer was the cells still present in the Cyto Buffer that were not used and left over from the sorting experiment. This was done to ensure no contamination and overall cell health was maintained. Untrapped cells were those cells that were not attracted to the Cytochip under the parameters used but rather flowed through the Cytochip and collected at the end of the device.

Overall, the health of the cells was not harmed during the cell sorting experiment. Once the parameters are met and plating is a continued success the project will move to using hMSCs to determine optimize the system to sort cells and determine what population of cell was sorted in the process.

APPENDIX D:
QPCR ANALYSIS OF DIFFERENTIATION AND TREATMENT OF HMSCS

Cycles Threshold (Ct) Data for Differentiation and Treatment Data

The following data is additional supporting data for qPCR analysis in Chapter 3 of this thesis. Based on the results below additional optimization of qPCR to determine how the gene expression is used by hMSCs that have undergone treatment. Both table D.1 and D.2 are representative CT data of high treatment samples of hMSCs.

Both data sets (Table D.1 and D.2) have three gene markers for adipogenesis (ADIPOQ, FABP4, and PPARG), three gene markers for osteogenesis (ALPL, COL1A1, and RUNX2), one stemness marker (SOX2), normalized control (GAPDH). These gene markers were used as there were proven to provide favorable results for the types of differentiation in tested same cell line hMSCs [17]. All gene markers are compared to the normalized control to determine up or down regulation of the gene.

Table D.1. Cycles threshold (Ct) Data for High Kifunensine (HK) treatments for specific gene-expression markers. AD refers to cells that have undergone adipogenesis, OS refers to cells that have undergone osteogenesis, and CTRL refers to cells that are considered controls that have not undergone treatment.

Differentiation Type	Gene Markers	TREATMENT TYPE				
		HK-AD	HK-OS	HK-CTRL	CTRL-AD	CTRL-OS
Adipogenesis	ADIPOQ	35.6	0.0	33.7	21.1	0.0
	FABP4	23.5	0.0	16.7	12.8	0.0
	PPARG	11.5	9.8	33.3	24.1	0.0
Osteogenesis	ALPL	0.0	11.4	32.7	0.0	29.0
	COL1A1	35.6	0.0	9.2	21.1	0.0
	RUNX2	0.0	33.1	31.0	0.0	32.7
Stemness	SOX2	24.2	24.2	27.0	26.7	25.9
Normalized Control	GAPDH	33.3	36.0	34.1	26.5	25.7

*NOTE: CTRL-CTRL cells (no treatment, no differentiation) were recorded as zero across all gene expression markers.

Table D.1 shows that HK-AD up regulated for ADIPOQ and COL1A1, while it down regulates for all others. HK-OS and HK-CTRL have no up regulation of any gene markers like the CTRL-CTRL sample. As noted, the CTRL-CTRL sample did not express any up regulation for any marker, which was expected since the sample did not receive any treatment or differentiation. Whereas the CTRL-AD demonstrates a slight up regulation for stemness but no up regulation for the expected adipogenic marker since the CTRL-AD underwent adipogenic differentiation. CTRL-OS as expected down regulated adipogenic for all three gene expression markers (0.0) and did up regulate for two out of the three osteogenic gene markers (ALPL and COL1A1).

Table D.2. Cycles threshold (Ct) Data for High N-Acetylglucosamine (HG) treatments for specific gene-expression markers. AD refers to cells that have undergone adipogenesis, OS refers to cells that have undergone osteogenesis, and CTRL refers to cells that are considered controls that have not undergone treatment.

Differentiation Type	Gene Markers	TREATMENT TYPE				
		HG-AD	HG-OS	HG-CTRL	CTRL-AD	CTRL-OS
Adipogenesis	ADIPOQ	35.6	0.0	29.7	21.1	0.0
	FABP4	0.0	11.8	23.5	12.8	0.0
	PPARG	36.3	0.0	21.3	24.1	0.0
Osteogenesis	ALPL	0.0	29.8	32.4	0.0	29.0
	COL1A1	35.1	0.0	29.7	21.1	0.0
	RUNX2	0.0	23.4	30.9	0.0	32.7
Stemness	SOX2	26.0	25.6	17.9	26.7	25.9
Normalized Control	GAPDH	31.2	27.4	29.7	26.5	25.7

*NOTE: CTRL-CTRL cells (no treatment, no differentiation) were recorded as zero across all gene expression markers.

In table D.2 HG-AD shows regulation for two out of the three adipogenic biomarkers (ADIPOQ and PPARG), and one osteogenic marker, COL1A1, when compared to the normalized control. Unsure how COL1A1 plays into HG-AD having an upregulation and additional testing may help determine if HG-AD is also expressing some osteogenic gene markers or the treatment conducted has also affected what is being expressed. As for HG-CTRL, up regulation of gene markers, ADIPOQ, ALPL, and RUNX2 were observed, which is also surprising noting that HG-CTRL only underwent treatment but no differentiation.

Below is visual representation of the gene expression for the distinct types of treatments conducted. All graphs were normalized using GAPDH as the housekeeper gene. Each graph represents a n =3 where each column being the type of treatment received. Values greater than zero represent genes that have been up regulated and vice versa.

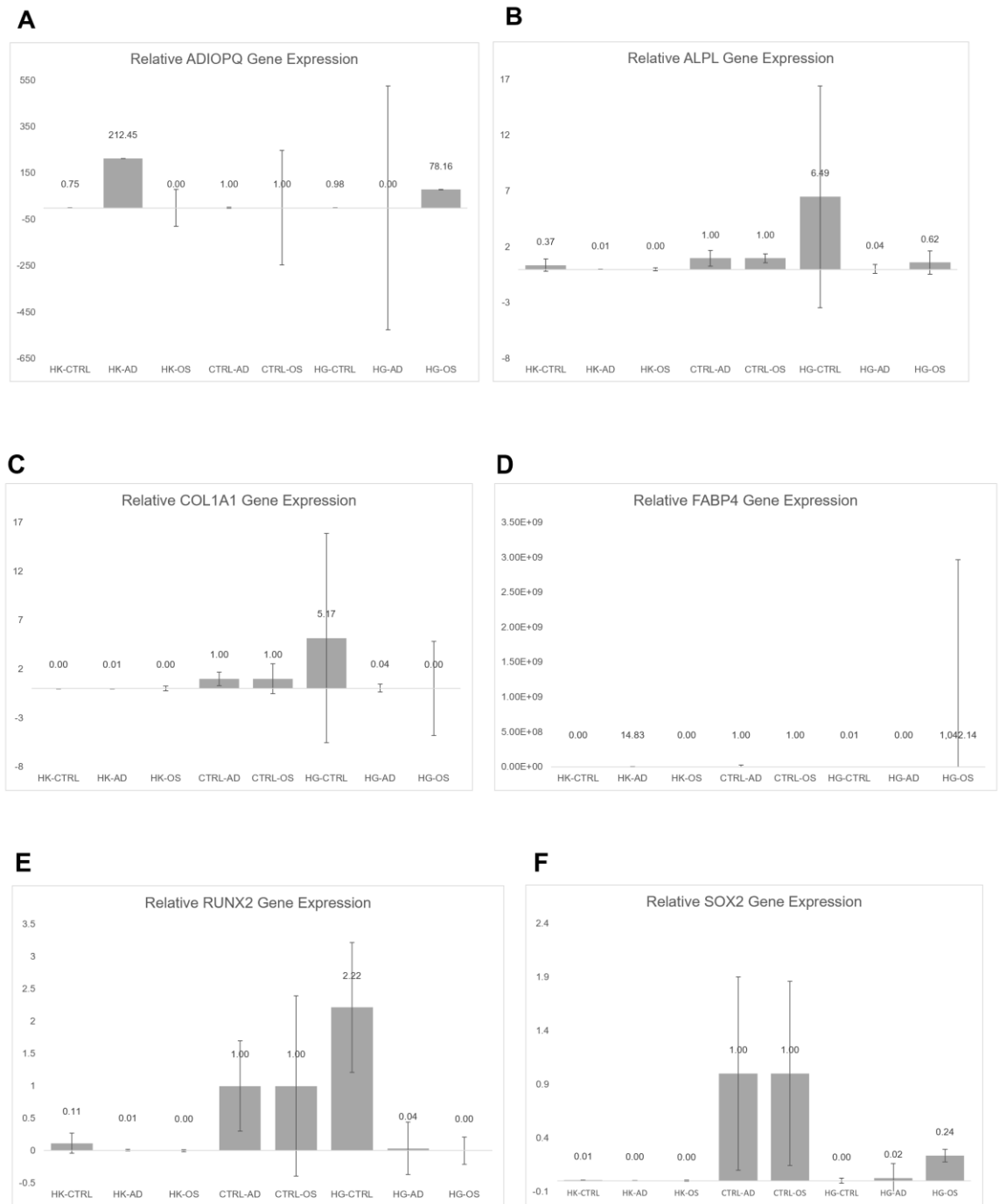


Figure D.1. Fold gene expression for AThMSCs that underwent treatment and differentiation (A-F). Where all the gene markers for adipogenesis (ADIPOQ, FABP4, and PPARG), three gene markers for osteogenesis (ALPL, COL1A1,

and RUNX2), one stemness marker (SOX2) were assessed to provide additional information on how the glycocalyx of the cell is affected by treatment and/or differentiation.

Graph D.1 (A) represents ADIOPQ gene expression for HK-AD and HG-OS were greater than the one which is up regulated. COL1A1 gene expression is upregulated by CTRL-AD, CTRL-OS, and HG-CTRL (D). FABP4 had no gene expression for any treated and/or differentiated by large error bars that express a processing error. RUNX2 gene expression was upregulated for CTRL-AD, CTRL-OS, HG-CTRL, HK-CTRL, HG-AD (E). More upregulation prevalent for HG-CTRL, CTRL-OS, CTRL-AD respectively (2.22, 1.00, 1.00).


SOX2 had gene expression for CTRL-AD and CTRL-OS, which confirms that without treatment (changes to the glycocalyx) stemness was not affected and in fact up regulated (F). Whereas all treated cells (HK-CTRL, HK-AD, HK-OS, HG-CTRL, HG-AD, HG-OS) did not express any stemness and therefore supports the theory that changes made the cells based on treated has affected something beyond what qPCR is able to demonstrate and other analysis into so the glycocalyx changes affect gene expression.

Although the data was collected to be processed as statistical data, it is apparent from the graphs that the more understanding on how the changes in the glycocalyx are affecting other changes that are related to how the gene are expressed. The data was not processed for additional statistical analysis as the error bars expressed were varying magnitude that would suggest high error due to a potential false positive for up regulation of some of the marker genes.

APPENDIX E:
PUBLICATION RIGHTS FOR IMAGES DISPLAYED

Figure 16. The Heterogeneity of MSCs, adapted from *Zha, K et. al. (2021)* [11].

8/10/23, 5:56 PM Rightslink® by Copyright Clearance Center



CCC
RightsLink

[Help](#) [Live Chat](#)

Heterogeneity of mesenchymal stem cells in cartilage regeneration: from characterization to application

Author: Kangkang Zha et al
Publication: npj Regenerative Medicine
Publisher: Springer Nature
Date: Mar 19, 2021
Copyright © 2021, The Author(s)

Creative Commons

This is an open access article distributed under the terms of the [Creative Commons CC BY](#) license, which permits unrestricted use, distribution, and reproduction in any medium, provided the original work is properly cited.

You are not required to obtain permission to reuse this article.
To request permission for a type of use not listed, please contact [Springer Nature](#)

© 2023 Copyright - All Rights Reserved | [Copyright Clearance Center, Inc.](#) | [Privacy statement](#) | [Data Security and Privacy](#)
| [For California Residents](#) | [Terms and Conditions](#) Comments? We would like to hear from you. E-mail us at customer-care@copyright.com

[https://is100.copyright.com/AppDispatchServlet?title=Heterogeneity of mesenchymal stem cells in cartilage regeneration%3A from characterization to ...](https://is100.copyright.com/AppDispatchServlet?title=Heterogeneity+of+mesenchymal+stem+cells+in+cartilage+regeneration%3A+from+characterization+to+...) 1/1

Figure 17. Cell Surface and Transcriptomic Comparison of “MSCs” from Different Tissues, adapted from *Sacchetti, B et. al.’s (2016)* paper [1].

8/10/23, 6:04 PM Rightslink® by Copyright Clearance Center

 Home Help Live Chat Sign In Create Account

No Identical “Mesenchymal Stem Cells” at Different Times and Sites: Human Committed Progenitors of Distinct Origin and Differentiation Potential Are Incorporated as Adventitial Cells in Microvessels



Author:
Benedetto Sacchetti, Alessia Funari, Cristina Remoli, Giuseppe Giannicola, Gesine Kogler, Stefanie Liedtke, Giulio Cassu, Marta Serafini, Maurizio Sampaolesi, Enrico Tagliafico, Elena Tenedini, Isabella Saggio, Pamela G. Robey, Mara Riminucci, Paolo Bianco

Publication: Stem Cell Reports
Publisher: Elsevier
Date: 14 June 2016

© 2016 The Authors.

Creative Commons Attribution-NonCommercial-No Derivatives License (CC BY NC ND)

This article is published under the terms of the [Creative Commons Attribution-NonCommercial-No Derivatives License \(CC BY NC ND\)](#). For non-commercial purposes you may copy and distribute the article, use portions or extracts from the article in other works, and text or data mine the article, provided you do not alter or modify the article without permission from Elsevier. You may also create adaptations of the article for your own personal use only, but not distribute these to others. You must give appropriate credit to the original work, together with a link to the formal publication through the relevant DOI, and a link to the Creative Commons user license above. If changes are permitted, you must indicate if any changes are made but not in any way that suggests the licensor endorses you or your use of the work.

Permission is not required for this non-commercial use. For commercial use please continue to request permission via RightsLink.

[BACK](#) [CLOSE WINDOW](#)

© 2023 Copyright - All Rights Reserved | Copyright Clearance Center, Inc. | [Privacy statement](#) | [Data Security and Privacy](#)
| [For California Residents](#) | [Terms and Conditions](#) Comments? We would like to hear from you. Email us at customercare@copyright.com

Figure 18. Schematic of how cell polarization and DEP response function in cells (adapted from Adams, T.N.G., et al., 2018 [15]).

8/21/23, 1:02 PM

RightsLink Printable License

ELSEVIER LICENSE
TERMS AND CONDITIONS

Aug 21, 2023

This Agreement between Cal state San Bernardino -- Romina Valentine Ico ("You") and Elsevier ("Elsevier") consists of your license details and the terms and conditions provided by Elsevier and Copyright Clearance Center.

License Number	5613810055322
License date	Aug 21, 2023
Licensed Content Publisher	Elsevier
Licensed Content Publication	Methods
Licensed Content Title	Separation of neural stem cells by whole cell membrane capacitance using dielectrophoresis
Licensed Content Author	Tayloria N.G. Adams, Alan Y.L. Jiang, Prema D. Vyas, Lisa A. Flanagan
Licensed Content Date	Jan 15, 2018
Licensed Content Volume	133
Licensed Content Issue	n/a
Licensed Content Pages	13
Start Page	91
End Page	103

<https://s100.copyright.com/AppDispatchServlet>

1/8

Figure 19. Visual representation of the positive and negative DEP responses based on changes in frequency (adapted from *Tunglin, Tsai, et al, 2021* [4]).

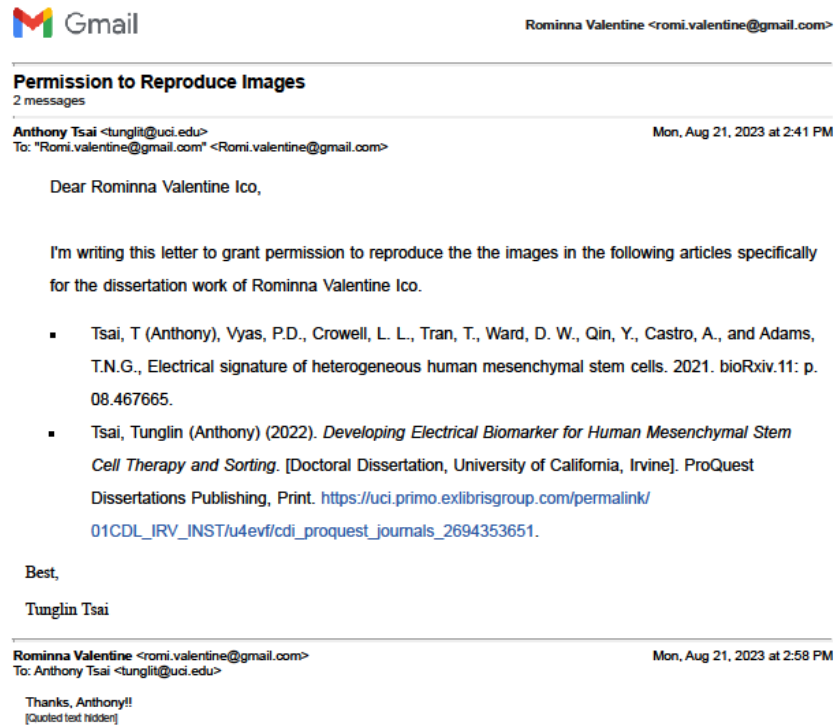


Figure 20. DEP Response Based on Frequency Changes, adapted from *Tsai, Tunglin (2022)* [17].

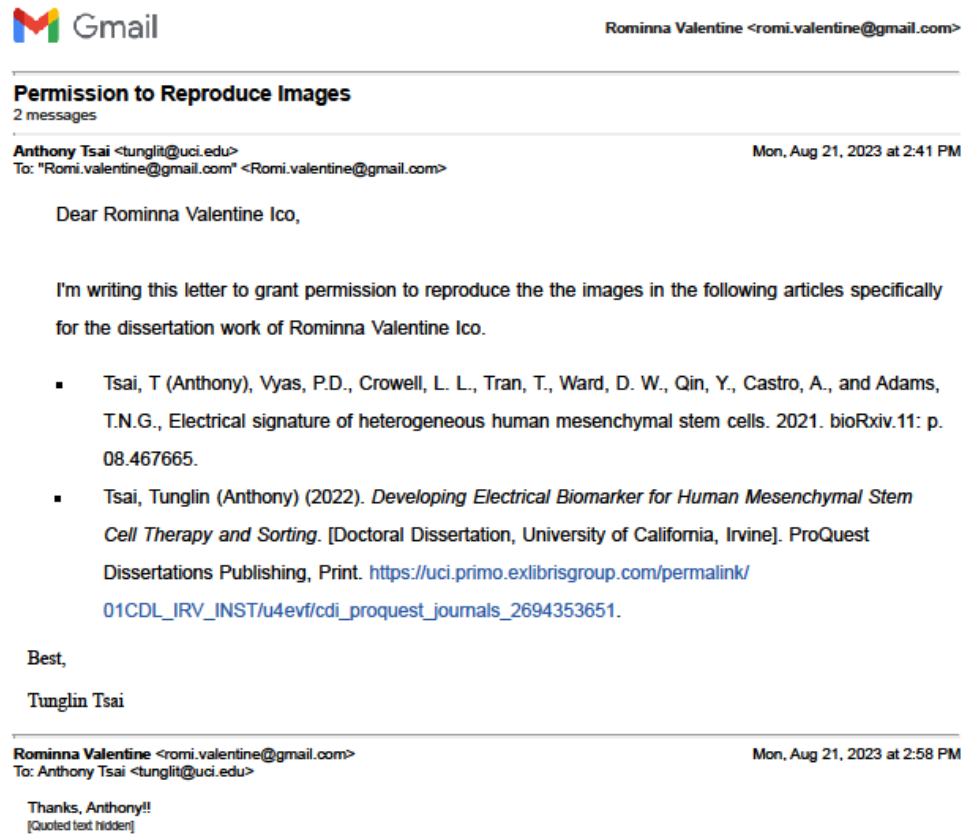


Figure 21. Representation of the glycocalyx complexity, from (Purcell, S, et al., 2019 [24]).

8/21/23, 1:32 PM marketplace.copyright.com/rs-uf-web/imp/license/7d3a879-abd2-46a7-8e69-0e0eabec2be4/49520904-ba79-4f2b-919b-6137e995...

CCC Marketplace

This is a License Agreement between Rominna Valentine Ico, Cal State San Bernarndino ("User") and Copyright Clearance Center, Inc. ("CCC") on behalf of the Rightsholder identified in the order details below. The license consists of the order details, the Marketplace Permissions General Terms and Conditions below, and any Rightsholder Terms and Conditions which are included below.

All payments must be made in full to CCC in accordance with the Marketplace Permissions General Terms and Conditions below.

Order Date	21-Aug-2023	Type of Use	Republish in a thesis/dissertation
Order License ID	1388496-1	Publisher	Royal Society
ISSN	2042-8901	Portion	Image/photo/illustration

LICENSED CONTENT

Publication Title	Interface focus	Country	United Kingdom of Great Britain and Northern Ireland
Author/Editor	Royal Society (Great Britain)	Rightsholder	The Royal Society (U.K.)
Date	01/01/2011	Publication Type	e-Journal
Language	English	URL	https://royalsociety.org/journals/

REQUEST DETAILS

Portion Type	Image/photo/illustration	Distribution	United States
Number of Images / Photos / Illustrations	1	Translation	Original language of publication
Format (select all that apply)	Print, Electronic	Copies for the Disabled?	No
Who Will Republish the Content?	Academic institution	Minor Editing Privileges?	No
Duration of Use	Current edition and up to 5 years	Incidental Promotional Use?	No
Lifetime Unit Quantity	Up to 499	Currency	USD
Rights Requested	Main product		

NEW WORK DETAILS

Title	DETERMINING THE EFFECTS OF GLYCOCALYX MODIFICATIONS ON THE ELECTROPHYSICAL PROPERTIES OF HUMAN MESENCHYMAL STEM CELLS	Institution Name	University of California, Irvine
Instructor Name	Tayloria N.G. Adams	Expected Presentation Date	2023-11-01

ADDITIONAL DETAILS

https://marketplace.copyright.com/rs-uf-web/imp/license/7d3a879-abd2-46a7-8e69-0e0eabec2be4/49520904-ba79-4f2b-919b-6137e995052b 1/7

Figure C.2. Schematic of the CytoChip provided by CytoRecovery interfaced with electronics and fluidics systems for the cell sorting experiment. Image rendering provided by *Hylar, A. (2021)* [32].

8/22/23, 11:53 AM

RightsLink Printable License

JOHN WILEY AND SONS LICENSE
TERMS AND CONDITIONS

Aug 22, 2023

This Agreement between Cal state San Bernardino -- Rominna Valentine Ico ("You") and John Wiley and Sons ("John Wiley and Sons") consists of your license details and the terms and conditions provided by John Wiley and Sons and Copyright Clearance Center.

License Number 5613830086274

License date Aug 21, 2023

Licensed Content
Publisher John Wiley and Sons

Licensed Content
Publication Electrophoresis

Licensed Content
Title A novel ultralow conductivity electromanipulation buffer improves cell viability and enhances dielectrophoretic consistency

Licensed Content
Author Eva M. Schmelz, Nathan S. Swami, Rafael V. Davalos, et al

Licensed Content
Date Apr 15, 2021

Licensed Content
Volume 42

Licensed Content
Issue 12-13

Licensed Content
Pages 12

<https://s100.copyright.com/CustomerAdmin/PLF.jsp?ref=4a0e4fb0-7060-4024-ae34-code8237c03f>

1/6

REFERENCES

- [1] B. Sacchetti *et al.*, “No Identical ‘Mesenchymal Stem Cells’ at Different Times and Sites: Human Committed Progenitors of Distinct Origin and Differentiation Potential Are Incorporated as Adventitial Cells in Microvessels,” *Stem Cell Rep.*, vol. 6, no. 6, pp. 897–913, Jun. 2016, doi: 10.1016/j.stemcr.2016.05.011.
- [2] F. H. Labeed *et al.*, “Biophysical Characteristics Reveal Neural Stem Cell Differentiation Potential,” *PLoS ONE*, vol. 6, no. 9, p. e25458, Sep. 2011, doi: 10.1371/journal.pone.0025458.
- [3] G. Fajardo *et al.*, “Bone marrow mesenchymal stromal cells from clinical scale culture: In vitro evaluation of their differentiation, hematopoietic support and immunosuppressive capacities,” *Exp. Hematol.*, vol. 44, no. 9, p. S70, Sep. 2016, doi: 10.1016/j.exphem.2016.06.128.
- [4] T. Tsai *et al.*, “Electrical signature of heterogeneous human mesenchymal stem cells,” *Bioengineering*, preprint, Nov. 2021. doi: 10.1101/2021.11.08.467665.
- [5] T. N. G. Adams, P. A. Turner, A. V. Janorkar, F. Zhao, and A. R. Minerick, “Characterizing the dielectric properties of human mesenchymal stem cells and the effects of charged elastin-like polypeptide copolymer treatment,” *Biomicrofluidics*, vol. 8, no. 5, p. 054109, Sep. 2014, doi: 10.1063/1.4895756.
- [6] T. N. G. Adams *et al.*, “Label-free enrichment of fate-biased human neural stem and progenitor cells,” *Biosens. Bioelectron.*, vol. 152, p. 111982, Mar. 2020, doi: 10.1016/j.bios.2019.111982.
- [7] E. López-Muñoz, “Células tumorales circulantes en cáncer de mama,” *Rev Med Inst Mex Seguro Soc*.
- [8] S. Grimnes, *Bioimpedance and bioelectricity basics*. Boston, MA: Elsevier, 2014.
- [9] K. C. Elahi, G. Klein, M. Avci-Adali, K. D. Sievert, S. MacNeil, and W. K. Aicher, “Human Mesenchymal Stromal Cells from Different Sources Diverge in Their Expression of Cell Surface Proteins and Display Distinct Differentiation Patterns,” *Stem Cells Int.*, vol. 2016, pp. 1–9, 2016, doi: 10.1155/2016/5646384.
- [10] L. A. Costa *et al.*, “Functional heterogeneity of mesenchymal stem cells from natural niches to culture conditions: implications for further clinical uses,”

Cell. Mol. Life Sci., vol. 78, no. 2, pp. 447–467, Jan. 2021, doi: 10.1007/s00018-020-03600-0.

- [11] K. Zha *et al.*, “Heterogeneity of mesenchymal stem cells in cartilage regeneration: from characterization to application,” *Npj Regen. Med.*, vol. 6, no. 1, p. 14, Mar. 2021, doi: 10.1038/s41536-021-00122-6.
- [12] J.-Y. Chen, X.-Z. Mou, X.-C. Du, and C. Xiang, “Comparative analysis of biological characteristics of adult mesenchymal stem cells with different tissue origins,” *Asian Pac. J. Trop. Med.*, vol. 8, no. 9, pp. 739–746, Sep. 2015, doi: 10.1016/j.apjtm.2015.07.022.
- [13] C. S. Chen† and H. A. Pohl, “BIOLOGICAL DIELECTROPHORESIS: THE BEHAVIOR OF LONE CELLS IN A NONUNIFORM ELECTRIC FIELD,” *Ann. N. Y. Acad. Sci.*, vol. 238, no. 1 Electrically, pp. 176–185, Oct. 1974, doi: 10.1111/j.1749-6632.1974.tb26787.x.
- [14] R. Pethig, “Review Article—Dielectrophoresis: Status of the theory, technology, and applications,” *Biomicrofluidics*, vol. 4, no. 2, p. 022811, Jun. 2010, doi: 10.1063/1.3456626.
- [15] T. N. G. Adams, A. Y. L. Jiang, P. D. Vyas, and L. A. Flanagan, “Separation of neural stem cells by whole cell membrane capacitance using dielectrophoresis,” *Methods*, vol. 133, pp. 91–103, Jan. 2018, doi: 10.1016/j.ymeth.2017.08.016.
- [16] J. Zhang, K. Chen, and Z. H. Fan, “Circulating Tumor Cell Isolation and Analysis,” in *Advances in Clinical Chemistry*, Elsevier, 2016, pp. 1–31. doi: 10.1016/bs.acc.2016.03.003.
- [17] Tsai, Tunclin (Anthony), “Developing Electrical Biomarker for Human Mesenchymal Stem Cell Therapy and Sorting,” Doctoral Dissertation, University of California, Irvine, 2022.
- [18] B. Alberts, *Essential cell biology*, Fourth edition. New York, NY: Garland Science, 2013.
- [19] M. J. Mitchell and M. R. King, “Physical Biology in Cancer. 3. The role of cell glycocalyx in vascular transport of circulating tumor cells,” *Am. J. Physiol.-Cell Physiol.*, vol. 306, no. 2, pp. C89–C97, Jan. 2014, doi: 10.1152/ajpcell.00285.2013.

- [20] J. L. Nourse *et al.*, “Membrane Biophysics Define Neuron and Astrocyte Progenitors in the Neural Lineage,” *Stem Cells*, vol. 32, no. 3, pp. 706–716, Mar. 2014, doi: 10.1002/stem.1535.
- [21] A. R. Yale *et al.*, “Cell Surface N-Glycans Influence Electrophysiological Properties and Fate Potential of Neural Stem Cells,” *Stem Cell Rep.*, vol. 11, no. 4, pp. 869–882, Oct. 2018, doi: 10.1016/j.stemcr.2018.08.011.
- [22] L. A. Flanagan *et al.*, “Unique Dielectric Properties Distinguish Stem Cells and Their Differentiated Progeny,” *Stem Cells*, vol. 26, no. 3, pp. 656–665, Mar. 2008, doi: 10.1634/stemcells.2007-0810.
- [23] P. Strzyz, “Bend it like glycocalyx,” *Nat. Rev. Mol. Cell Biol.*, vol. 20, no. 7, pp. 388–388, Jul. 2019, doi: 10.1038/s41580-019-0142-2.
- [24] S. C. Purcell and K. Godula, “Synthetic glycoscapes: addressing the structural and functional complexity of the glycocalyx,” *Interface Focus*, vol. 9, no. 2, p. 20180080, Apr. 2019, doi: 10.1098/rsfs.2018.0080.
- [25] M. L. Huang, R. A. A. Smith, G. W. Trieger, and K. Godula, “Glycocalyx Remodeling with Proteoglycan Mimetics Promotes Neural Specification in Embryonic Stem Cells,” *J. Am. Chem. Soc.*, vol. 136, no. 30, pp. 10565–10568, Jul. 2014, doi: 10.1021/ja505012a.
- [26] L. Möckl, “The Emerging Role of the Mammalian Glycocalyx in Functional Membrane Organization and Immune System Regulation,” *Front. Cell Dev. Biol.*, vol. 8, p. 253, Apr. 2020, doi: 10.3389/fcell.2020.00253.
- [27] S. Reitsma, D. W. Slaaf, H. Vink, M. A. M. J. Van Zandvoort, and M. G. A. Oude Egbrink, “The endothelial glycocalyx: composition, functions, and visualization,” *Pflüg. Arch. - Eur. J. Physiol.*, vol. 454, no. 3, pp. 345–359, Jun. 2007, doi: 10.1007/s00424-007-0212-8.
- [28] Y. Xiong, Q. Li, M. Kailemia, C. Lebrilla, S. Nandi, and K. McDonald, “Glycoform Modification of Secreted Recombinant Glycoproteins through Kifunensine Addition during Transient Vacuum Agroinfiltration,” *Int. J. Mol. Sci.*, vol. 19, no. 3, p. 890, Mar. 2018, doi: 10.3390/ijms19030890.
- [29] V. J. Coulson-Thomas, T. F. Gesteira, V. Hascall, and W. Kao, “Umbilical Cord Mesenchymal Stem Cells Suppress Host Rejection,” *J. Biol. Chem.*, vol. 289, no. 34, pp. 23465–23481, Aug. 2014, doi: 10.1074/jbc.M114.557447.
- [30] A. D. Elbein, J. E. Tropea, M. Mitchell, and G. P. Kaushal, “Kifunensine, a potent inhibitor of the glycoprotein processing mannosidase I.,” *J. Biol.*

Chem., vol. 265, no. 26, pp. 15599–15605, Sep. 1990, doi: 10.1016/S0021-9258(18)55439-9.

- [31] K. Macharoen *et al.*, “Effects of Kifunensine on Production and N-Glycosylation Modification of Butyrylcholinesterase in a Transgenic Rice Cell Culture Bioreactor,” *Int. J. Mol. Sci.*, vol. 21, no. 18, p. 6896, Sep. 2020, doi: 10.3390/ijms21186896.
- [32] A. R. Hyler, D. Hong, R. V. Davalos, N. S. Swami, and E. M. Schmelz, “A novel ultralow conductivity electromanipulation buffer improves cell viability and enhances dielectrophoretic consistency,” *ELECTROPHORESIS*, vol. 42, no. 12–13, pp. 1366–1377, Jul. 2021, doi: 10.1002/elps.202000324.